INVESTIGATION OF RF RADIATION
AS A SECONDARY PHENOMENON
FOR USE IN CHECKOUT

James W. Ballard

Systems Research Laboratories, Inc.

Eugene F. Horn

Systems Research Laboratories, Inc.

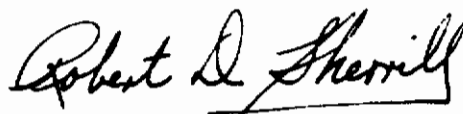## FINAL TECHNICAL DOCUMENTARY REPORT AFAPL-TR-65-46

June 1965

FOREWORD

The report was prepared by Systems Research Laboratories, Inc., Dayton, Ohio, as the final phase of Contract AF33(615)-1489, under task No. 811925, Project 8119, "Investigation of Secondary Phenomena for Use in Checkout." The work was performed under the direction of the Air Force Aero Propulsion Laboratory, Research and Technology Division, Air Force Systems Command. Mr. David A. Barnhardt was project engineer for the Air Force.

The study was begun in October 1962 and was completed with the publication of this report. The overall study was under the direction of Dr. James W. Ballard. Dr. Eugene F. Horn contributed substantially to the program. Mr. David Patti gave invaluable assistance in the initial part of the program. Mr. Thomas O. Apple contributed in many ways to the experimental portions of the program.

This report, AFAPL-TR-65-46, concludes the work on Contract AF33(615)-1489.

This report was submitted by the authors in June, 1965.

This technical report has been reviewed and is approved.

ROBERT D. SHERRILL, Chief
Ground Support Branch
Technical Support Division

ii

ABSTRACT

The emission of radio-frequency (rf) radiation has been studied over a range of frequencies from .15 to 400 megacycles per second (Mc/sec) for small gaps of .5 to 10 mils. The electrodes were .050-inch in diameter with polished plane ends which formed the gap. Most of the work reported was done in air at atmospheric pressure with nickel electrodes although argon gas and gold, aluminum, and copper electrodes were employed.

Considerable attention was given to shielding, and the effect of receiver and generator circuitry. The effect of antennas and cables were also studied in relation to rf radiation emission and reception.

Peaks were found in the rf radiation spectrum from 6 Mc/sec to 400 Mc/sec. Peaks with rather exact harmonic frequency relationships came from the circuitry, other peaks did not have this exact relationship. Very simple generator and receiver circuits were employed. Very good repeatability of rf radiation measurements was obtained.

Radiation from malfunctioning systems is attributed to a brush type discharge across very small discontinuities within the electrical parts. These discontinutities in a number of cases were found to be essentially contact, i.e. less than a few thousand angstroms. Some of the discontinuities and discharges were not visible to the unaided eye; however, rf radiation was emitted. Effects studied in larger gaps, .5 to 10 mil range, were correlated with the phenomena in the component discontinuities. The mechanism causing breakdown was found to be the avalanche type with the involvement of secondary electronic emission. The spectral peaks were found with a spectrum analyzer. Each peak is interpreted as the envelope of electron energy distribution. The experimental evidence indicates electrons are situated in both the gas discharge and in the external circuitry. Other characteristics of the discharge are given.

Radio-frequency spectral radiation peaks and background were demonstrated as arriving from discontinuities in electrical devices. These devices include cold soldered joints, transistors, diodes,

iii

potentiometers and film type resistors. No rf radiation was obtain-
ed from carbon resistors, though it was obtained from film type resist-
ors. Radio-frequency radiation was obtained from graphite. (Note:
carbon is amorphous; graphite is carbon in a crystalline state).
No rf radiation was obtained from the vacuum tubes tested.

TABLE OF CONTENTS

LIST OF ILLUSTRATIONS

LIST OF ILLUSTRATIONS
(continued)

LIST OF ILLUSTRATIONS
(continued)

LIST OF TABLES

Section 1

INTRODUCTION

Under Air Force Contract 33(657)-9913, numerous physical laws and effects were investigated to determine the feasibility of using various secondary phenomena for the checkout of electronic circuitry.[1] The term "secondary phenomena" refers to the characteristic emissions from operating electronic circuitry or components thereof. During the investigation of secondary phenomena, Systems Research Laboratories, Inc. personnel determined that the use of radio-frequency (rf) phenomenon for detection of malfunctioning of electronic components and circuitry was one of the more promising phenomena. This rf radiation was found to be detectable by either direct methods, sensors placed in close proximity to the components, or by detecting reflected radiations in the power supply leads.

SRL personnel discovered rf radiation emanating from several pieces of equipment and numerous electronic components by use of a radio receiver monitoring the rf emissions appearing in the power leads. During the progress of this program, it was found that Minneapolis-Honeywell was also working on this phenomenon.[2]

It was found that the electronic components or circuitry had to be sharply tapped to cause potential malfunctioning components, soldered joints and other electrical connections to emit rf radiation. It was, therefore, postulated that electrical discontinuities existed in the malfunctioning parts, and that a sharp tap caused the discontinuity to open sufficiently to permit a microscopic electrical discharge.

It was further postulated that the discontinuities in electrical parts could be represented by an electrical discharge between closely spaced electrodes. A discontinuity is defined as a gap or break in the electrical circuit. It is envisioned these discontinuities or gaps are of the order of 10^{-5} to 10^{-1} centimeter (cm). Gaps of the order of 10^{-4} cm are found in electrical contacts when they are made.[3] Gaps of these very small dimensions are difficult to operate and maintain stable. Those in the small range 1.3×10^{-3} to 5.4×10^{-3} cm (.5 to 10 mils) are less difficult to operate. It was anticipated that the results of a study of prebreakdown phenomena of small gaps could be correlated with the prebreakdown phenomena of very small

1

gaps. This was later found to be the case. It is demonstrated later on in the experimental work. Thus, a study of the prebreakdown phenomena in small gaps will be employed to interpret the phenomena occurring in the very small discontinuities of electronic systems.

SRL tested some solid state modules from a computer and found in one case a transistor which emitted rf radiation at 25 mega-cycles per second (Mc/sec). This was in accord with the frequency found in reference (1). On 9 July 1963, SRL set up electrical discharge gaps of .002 and .022 inch and obtained rf peaks at 27.5 and 14.6 Mc/sec and also at lower frequencies. The radiation was captured by an antenna close to the discharge and analyzed with a short wave-length receiver. Later, it was shown the radiation could also be detected with a coil of wire wrapped around the power supply lead of the discharge. A spectrum analyzer indicated each peak, Figure 1.

The source of these phenomena were not specifically known, nor their exact nature understood. The objective of the present work is to determine the nature of the phenomena and its applicability to the check out of electronic circuitry. The following report will cover problems in instrumentation, making reliable rf measure-ments, and experimental work explaining some of the experimental phenomena. This work is somewhat exploratory, although a deter-mination of a more satisfying interpretation of the source of rf radiation has been made.

In each case:

Arc Gap 0.002 inches
Arc Voltage 1560 volts
Arc Current 6.3ma

Mv

$\frac{1}{25}$ sec

19mc   25mc   29mc

Mv

$\frac{1}{10}$ sec

20mc   25mc   30mc

Mv

1 sec

20mc   25mc   30mc
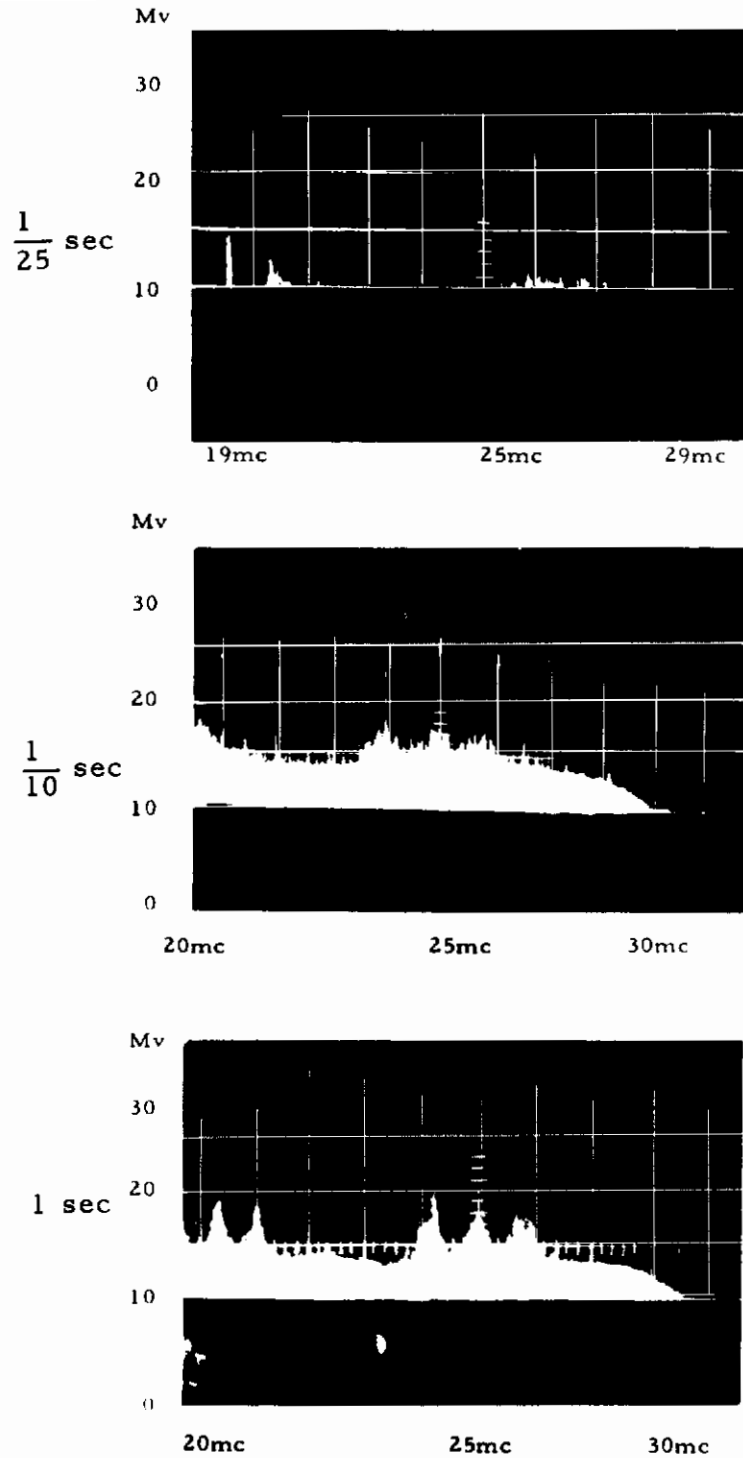
Figure 1. Frequency Spectrum for Different Exposure Times

3

Section 2

THEORY

The discharge between the electrodes may take place in several distinct steps.[4] Increasing the potential and current from zero across the electrodes the following types of discharges may exist:

1. Dark Discharge
2. Glow Discharge
3. Brush Discharge
4. Spark Discharge
5. Arc Discharge

The relative magnitudes of potentials and currents for these dis-charges are shown in Figure 2.

The electrical discharge may consist of electrons, negative ions, positive ions, metastable and neutral atoms. Ions are genera-ted by a collision of the particles. Townsend's equation for the total number of ions generated is

$$n = n_o \frac{(\alpha - \beta)\,\epsilon^{(\alpha - \beta)d}}{\alpha - \beta\,\epsilon^{(\alpha - \beta)d}} \qquad (1)$$

where: n_o is the number of ions generated per second at the negative electrode; α is Townsend's first coefficient and is defined as the number of ions which a single negative ion produces by collision in 1 cm of its path; β is Townsend's second coefficient and is defined as the number of ions formed by a positive ion by collision for each cm of its path through the gas, and d is the distance between electrodes (parallel planes).

The values of β are usually small compared with those of α except for large fields and large values of d. In general, a positive ion is a molecule of gas which has lost an electron from its outer shell while the negative ion is probably the electron. The

4

a - Dark Discharge
b - Glow Discharge
c - Brush Discharge
d - Spark Discharge
e - Arc Discharge
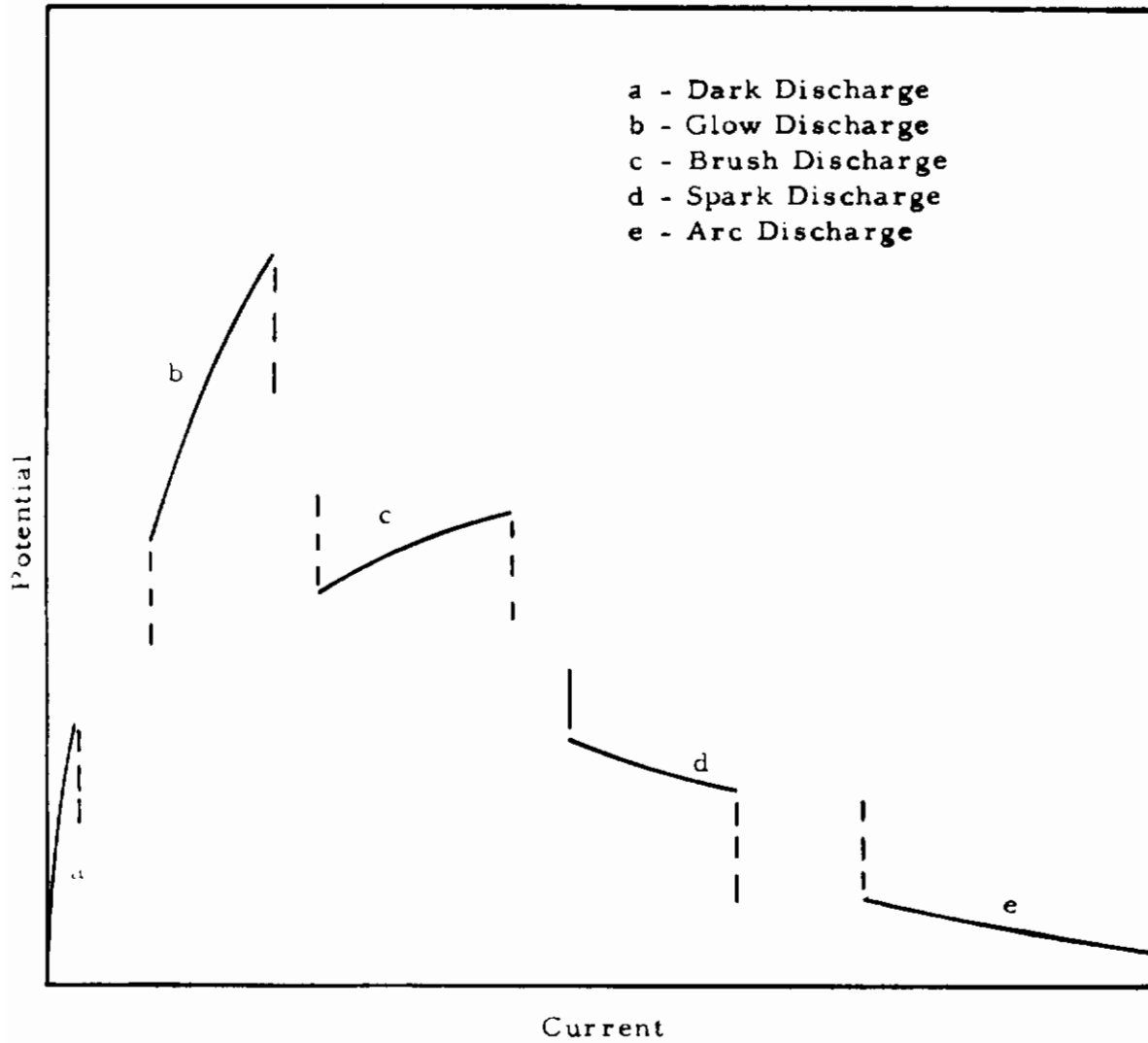
Potential

Current

Figure 2.   - Potential-Current Curves for Discharges Between
Electrodes.

mass of the electron is 9.107×10^{-28} gram; the mass of an argon atom is 6.63×10^{-23} gram. Thus, for a given amount of energy (having the same charge), the efficiency of a particle as an ionizing agent decreases rapidly as the size of the particle is increased.

THE SPARK

It is evident from Eq 1 that the number of ions produced, n, or current, would become infinite if the denominator became zero, i.e.,

$$\alpha = \beta_{\epsilon}^{(\alpha - \beta)d}$$

This equation describes the spark discharge. If $d = S$ and X is the field for this distance, the sparking potential is given by XS. (V/S is the field). If the gas pressure between electrodes is varied, it will be found that there is a critical pressure for which the sparking potential is a minimum. Paschen's Law states the sparking potential V depends only on the mass M of gas between the electrodes; that is, the pressure and the gap separation, ps. This law is true for all pressures both above and below the critical pressure.

THE BRUSH DISCHARGE

This type of discharge is found if the conductors are small and are separated by considerable distances so that the fields between electrodes are far from uniform. A luminous brush is formed on the portion of the conductor where the field is most intense, fading away as the distance from the electrode increases. It consists of a number of small sparks commencing at the electrode and terminating in air. The minimum potential required to start a brush discharge from a point electrode depends upon the sign of the point; the potential being greater for a positive point than for a negative point. If the point is negative, positive ions are moving toward it and produce electrons by collision with molecules of the gas, and by collision with the electrodes. If the point is positively charged only the first of these sources are available.

THE DARK DISCHARGE

For example, the discharge between a point and plane frequently commences and can be measured with a sensitive galvanometer

6

or electrometer before any sign of luminosity. If the potential is increased, a glow forms on the point and frequently a brush discharge may be formed. If the current is increased sparking takes place and further increase in current may produce an arc.

THE ARC DISCHARGE

In the case of the arc discharge, electrons carrying the current come mainly from the electrodes which become intensely hot, and emit electrons thermally rather than those which are formed by collision of molecules of gas in the spark and brush discharges. It has been found that this type of discharge does not emit rf radiation.

FIELD EMISSION

In addition to the electrons produced thermally by a hot body, electrons may be produced by a field emission; that is, by the potential that exists between two electrodes, the field being V/d(volts/cm) $=$ E. A very good description of the basic processes involved is given by A. L. Ward.[5] Although strong electrical fields cannot ionize atoms or molecules directly, comparatively small fields can accelerate electrons already present in the gas to sufficient velocity to ionize atoms by collision. Free electrons will be present in the gas because of the reaction of the gas to cosmic rays, light, the photoelectric effect, possible radioactivity, etc. A potential applied across parallel plates, for example, will produce a drift velocity for the electron and positive ion proportional to the field. Though the electron has thermal energy and zig-zags across the gap, if the applied field is sufficient, it gains enough energy to ionize the gas in the gap, creating a new electron and a positive ion. The positive ion proceeds slowly to the cathode, but the new electron will also be able to ionize creating a chain reaction known as the Townsend Avalanche.

Gas ionization alone (except at high over-voltages) is not sufficient for breakdown. Secondary processes are also required. These include the liberation of electrons from the cathode by bombardment of positive ions, photons, and metastable (long-life excited) atoms. Loeb[6] lists these secondary mechanisms symbolically as γ_i, γ_p, and γ_m respectively. From these basic processes, electrical breakdown may be calculated and characteristics of the discharge studied.

STREAMER THEORY OF SPARK BREAKDOWN

A type of electrical discharge pertinent to the studies made is spark breakdown due to streamers. The streamer theory will be briefly reviewed.

General Description

Streamers are branch-like discharges which look like lightning discharges. There is a main trunk with many branches and "fingers." The streamer theory involves positive ion space charges, electron avalanches, the production of electrons by collision processes, field emission at the cathode, and from the photoelectric effect of the progressing positive ion charge as it emits photons (light particles of hv energy). The photoelectrons are emitted by gas atoms or molecules and by the cathode. If Figure 3 is followed closely, the explanation of the mechanism will become more apparent.

Explanation of the Discharge Phenomena

The streamer discharge occurs just before spark breakdown. The mechanism describing this phenomena is based upon the dishcarge between positive point and negative plane separated by 2 to 5 cm in an atmosphere of air with square wave pulsed potentials on the electrodes, Figure 3. [7-10] The essential difference in these experiments and SRL's experiments is the discharge gap length and the application of a square wave potential. The gaps used in this program are very small, representing discontinuities in components and instead of pulsed, constant potentials are applied.

Positive Streamers

Positive ions and electrons usually exist in a discharge gap before a potential is applied to the electrodes. These ions and electrons may have been produced by cosmic rays, the photoelectric effect of ambient light on the gas atoms, molecules and/or cathode, x-rays, or other types of radiation. The application of a positive pulse to the point electrode, Figure 3, will attract electrons. These electrons will produce positive gas ions. This occurs when high velocity electrons collide with molecules, knocking an electron from its orbit. Since one electron, in general, is knocked from the molecule (other electrons may become excited to outer orbits), it becomes a

8
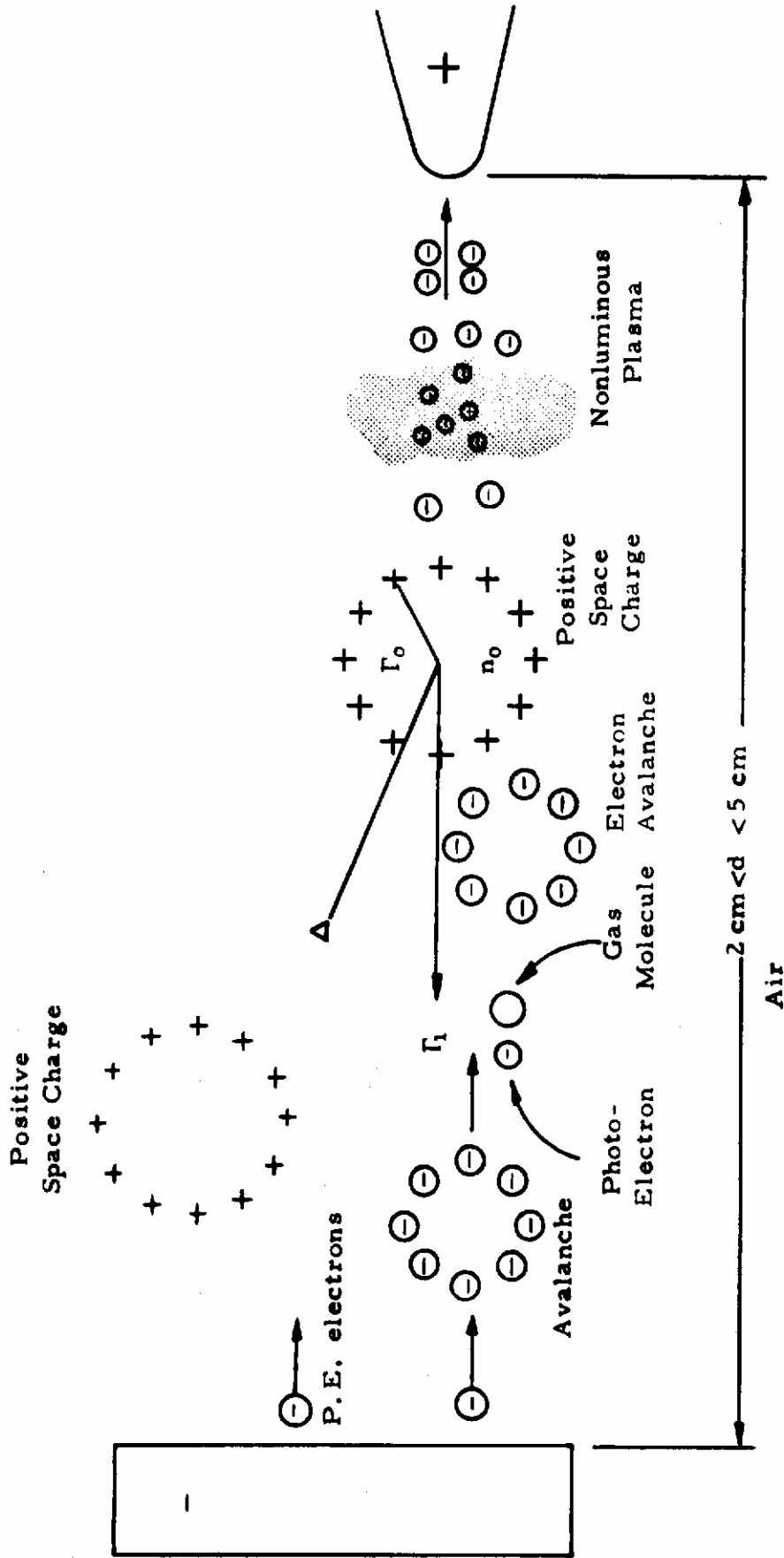
n_0 = number of ions in a positive space charge, $\sim 10^8$ ions

r_0 = radius of positive ion space charge, $\sim 2.85 \times 10^{-3}$ cm

r_1 = electron avalanche started by photoelectrons, $\sim .025$ cm

Δ = position of new positive space charge created by an electron avalanche formed at r_1, $\sim 6 \times 10^{-3}$ cm

Figure 3. Diagram for Explaining the Mechanism of Streamer Theory of Spark Breakdown

9

positive ion with a positive charge equal to that of the lost electron.
It has been shown that the positive ions, after repulsion from the
positive electrode, form spherical positive space charges[7] near
the positive point electrode, Figure 3. The radius for this space
charge is in one case 2.85×10^{-3} cm. This positive space charge
leaves a nonluminous plasma, or an electrically conducting gas
behind it as it moves away from the anode. Electrons dropping back
into the lower energy orbits of the excited positive ions result in the
emission of light. This light, or photons, produce photoelectrons
in the gas in the region Δ, Figure 3. One of the photoelectrons
will ionize a gas molecule. The two resulting electrons will ionize
two more gas molecules resulting in four electrons and so on in
geometric progression. An electron avalanche will be produced in
a very short time which moves toward the anode. At the same time,
the positive space charge slowly disintegrates and a new positive
space charge of ions will form at the region Δ, Figure 3. A sequence
of positive space charges leaving the anode will manifest itself as
visible streamers. These streamers were studied with the use of
photographic film. The tips of these streamers are at high potential
because of their charge plus the extension of the field applied to the
anode which connects to the streamer ends through the nonvisible
conducting gaseous plasma and streamers, Figure 3. As the positive
space charge approaches the cathode, particularly for smaller gaps,
photoelectrons plus field emission electrons are emitted from it;
these electrons form an electron avalanche which travels toward the
anode.

This simple description interprets the streamers as adding
their fields to the existing fields by the positive space charges
created. These positive space charges are created by electron
avalanches and photoelectric ionization of the gas ahead of the advancing
streamer tip. Since the path between the anode and cathode is now
electrically conducting, electron avalanches created at the cathode
will proceed rapidly along this path toward the anode causing the
breakdown. This is called the return stroke from the cathode.

Negative Streamers

The avalanche of photoelectrons and field emission electrons
travel from the cathode. The photoelectrons produced by these
avalanches jump ahead of the parent avalanches and produce further
avalanches. The positive space charge rapidly attenuates and joins

10

the original electrons in the original avalanche. This process is repeated as the anode is approached. A high applied or guiding field applied to the electrodes will be of more importance to the negative streamers, than for the positive streamers. It was found that the anode directed streamer was not easy to create and is best observed in overvoltage uniform fields. It has been studied with photographic film used as a detector.

THE BRUSH DISCHARGE

Importance of the Brush Discharge

Of the five types of discharge mentioned above, the brush type electrical discharge was found important in emanating rf radiation (electromagnetic radiation). The radiation occurs at a lower gap potential than the spark and would, therefore, occur before the spark in malfunctioning electronic components. Should a spark occur in a component or circuit, it would be quite obvious there was a malfunction present. It is, therefore, important to study the brush type discharge because it has been found present in small discontinuities in electronic parts and because it can be produced in very small gaps between electrodes.

Description of Discharge

The electrodes consisted of wires .050-inch in diameter, usually with plane polished ends, and a gap between .0005 to .010 inch. The current was usually limited to a maximum of 50 microamperes, with potentials available from a regulated power supply to 4000 volts dc or up to 2000 volts dc battery.

As the potential is slowly increased across the gap, a threshold potential is reached at which a single electrical pulse is obtained. As the potential is increased, the pulse rate increases. A pulse, or electrical discharge, is identified as a single trace on the oscilloscope, Figure 4; a count on the electronic counter; a click from the speaker of a short wave (rf) receiver at any frequency on its range; as a rf noise background on the noise meter over the frequency range and with a series of peak frequencies; or background noise over the frequency range of the spectrum analyzer. The peaks on the latter instrument become apparent if the suspected position of peaks is photographed over a short period of time or

11
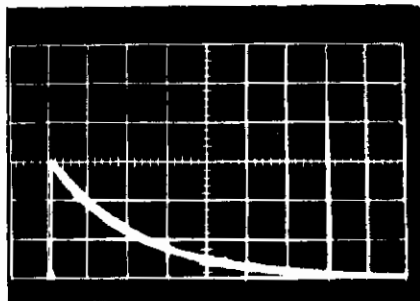
Figure 4.   Oscilloscope Record Showing Rapid Rise Time and Decay of Electrical Pulses Between Copper Electrodes Separated 001 Inch, in Air at a Pressure of 730 Torr, Power Supply Voltage 2300 VDC, 10 Microsecond/cm Horizontal Scale, 2 Volts/cm Vertical Scale, 2500 Spikes/second, Resistances Shown in Figure 6.
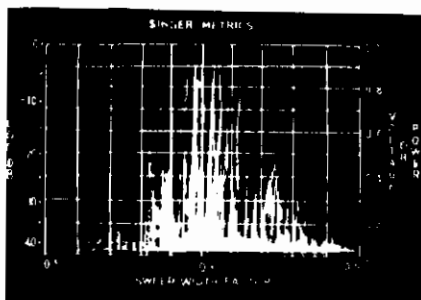
Figure 5.   Discrete Frequency Group, or Peak, at 21.5 Mcps for Copper Electrodes Separated 001 Inch in Air at a Pressure of 730 Torr, Power Supply Voltage 2300 VDC, Limiting Current Resistor 80 Megohms, Band 5 Mcps Wide.

12

if the gap potential is increased. A single low voltage rf peak is shown in Figure 5 indicating the formation of a peak by photographic integration. The circuit of linear elements is shown in Figure 6. Circuitry will be discussed under "Experimental" in this report.

Gaseous Phenomena

With the data to be subsequently discussed, it appears reasonable for one interpretation to regard each electrical pulse of the brush type discharge as a single avalanche. An avalanche is defined as the cumulative process in which charged particles accelerated by an electric field produce additional charged particles through collision with neutral gas molecules or atoms. An avalanche exists in a Townsend discharge when the applied voltage across the gap is sufficient to cause electrons to ionize gas molecules upon collision, thus releasing new electrons. The equation describing the formation of an avalanche, given above is

$$n = n_o e^{\alpha x}$$

where for a single avalanche n_o = one electron, α is Townsend's first coefficient and is defined as a number of ions which a single negative ion (or electron) produces by collision in 1 cm of its path and x is the distance traveled by the negative ion. This equation is used when the homogenous field E is large in comparison to the space charges of electrons and ions. An avalanche is made visible by a cloud chamber technique.[11] One such avalanche is presented in Figure 7. A square wave of voltage V reacts on an electron "e" and an avalanche is produced. After the time T, the electrical field disappears so that production of electrons stops and they attach to molecules. The **drift** path l of the avalanche within the gap is

$$l = v_- T$$

where v_- is the drift velocity of electrons, and l is shorter than the gap distance, d. In air v_- is about 10^7 cm/sec; d = 3 cm; T must be $<3 \times 10^{-7}$ sec. During this time, the positive ion with a much lower drift velocity of about 10^{-5} sec remains relatively fixed and the electrons move with velocity forming the head buildup with the long positive tail. The form of the track is wedge shape because
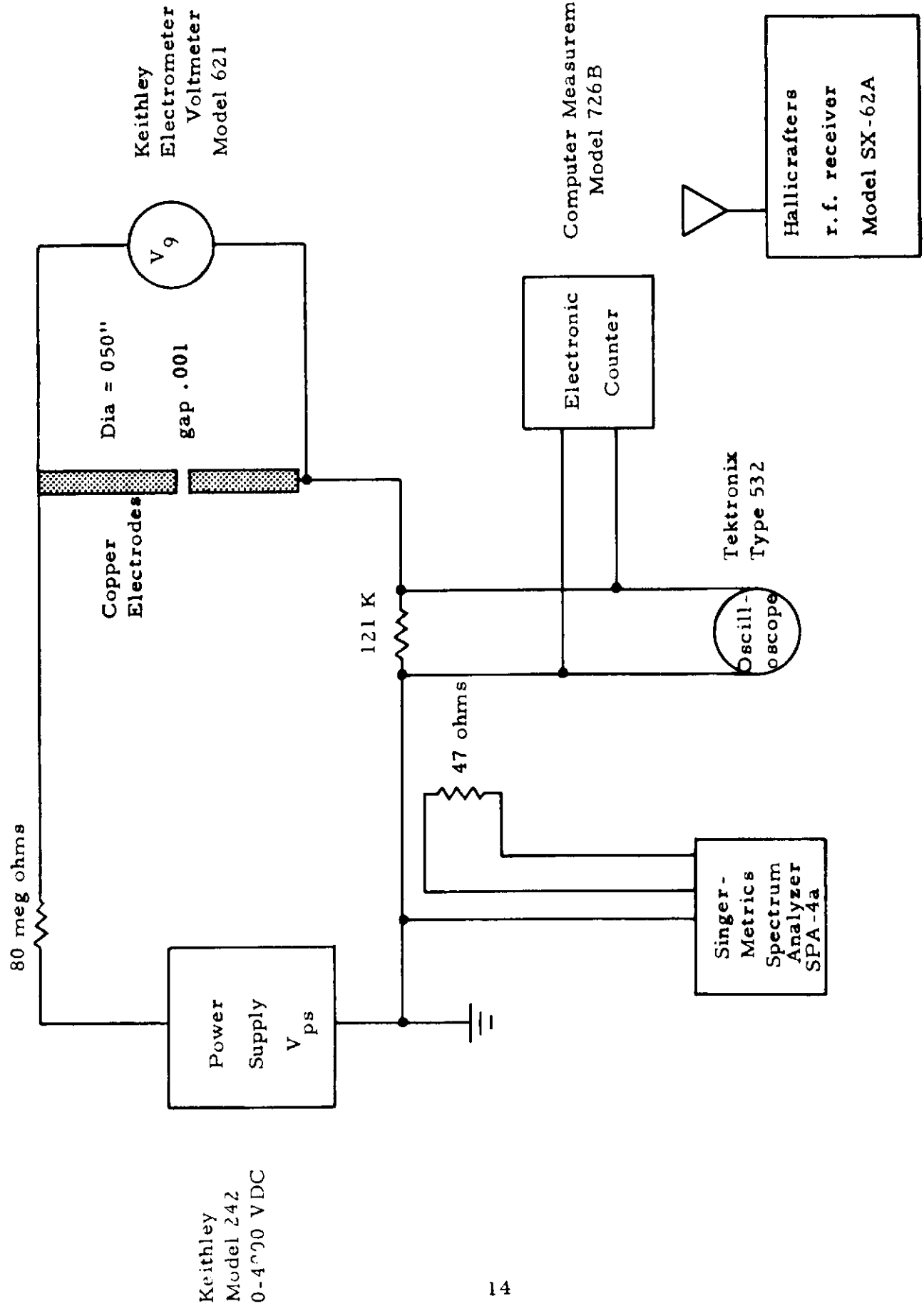
13

Figure 6. Electric Discharge Circuit and Instrumentation

14
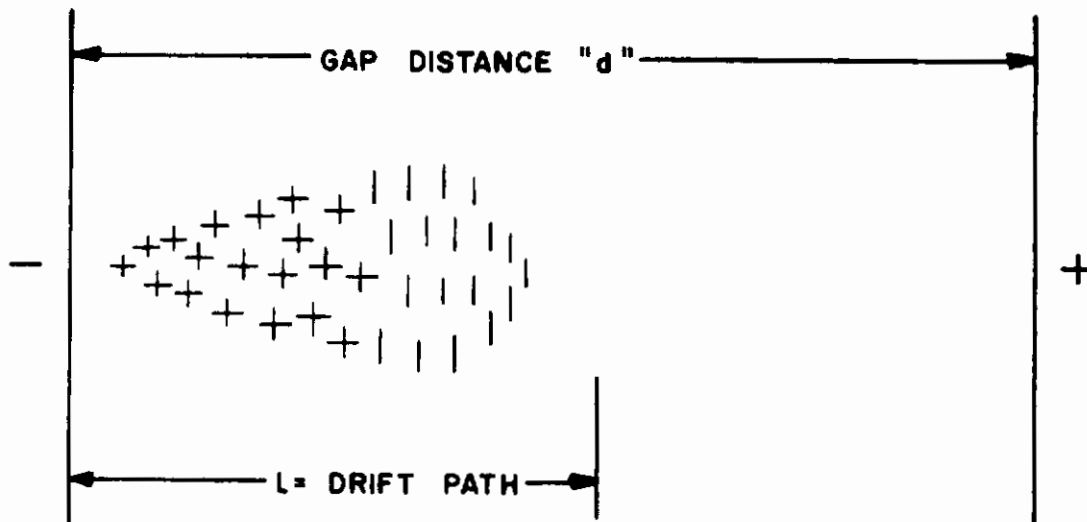
Figure 7. Distribution of Carriers in an Avalanche Produced
by a Square Wave of Voltage of T Sec Duration. Such
Avalanches are Made Visible by the Cloud Chamber
Method.[11]

15

of thermal diffusion of the electron group heated by the acceleration in the electrical field. The head of the avalanche is rounded due to diffusion of electrons in all directions. The profile is greatly changed for the electron density $n > 10^7$. Such avalanches are made visible by the cloud chamber method discussed in reference 11. Thus, for a single avalanche in N_2 at 280 torr, a gap of 3.6 cm, an impressed voltage 250 volts, the avalanche has started in a time interval of 1 nanosecond (nsec). [12]

The above discussion conveys an idea of avalanches under the conditions enumerated. The experimental conditions of the electrical discharges in the work that follows are considerably different employing air at atmospheric pressure between .050 inch diamenter plane electrodes polished and separated .0005 inch to .010 inch. The electric fields, E, were of the order of $200 \times 10^3 \frac{\text{volts}}{\text{cm}}$ and

$\frac{E}{p} \sim 320 \frac{\text{volts}}{\text{cm torr}}$ where p is the pressure of air between the gap.

Figure 8 is a photomicrograph of a type of discharge between .050-inch diameter copper electrodes, polished plane on the ends. The gap separation is .0114 inch, the width of the discharge column .0145 inch and the diameter of the largest sphere of light on the cathode is .0009 inch. The gap was in series with a battery potential of 1035 volts and a series resistance of 1.5 megohm. An electronic counter recorded 100 counts/second; that is, 100 electrical discharges/second. For the present, if it is assumed the spheres of light on the cathode are avalanches, a comparison of avalanche diameters can be made approximately; Table 1. Further work will probably disprove this assumption. The nature of the brush discharge depends considerably upon the value of the current limiting resistor. Therefore, as will be seen later, Figure 8 is representative of only a brush discharge under certain conditions.

Table 1

Comparison of Avalanche Diameters			
	2r (cm)	E ($\frac{KV}{cm}$)	p (torr)
SRL	.0025	200	730
Raether[11]	.22	11.8	273

16
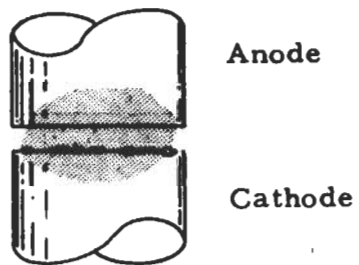
Figure 8.   Photomicrograph of a Discharge Between .050 Inch
Diameter Copper Electrodes with Polished Plane Ends with
.0114 Inch Gap.   Light Spheres on the Cathode are .0009 Inch.
Battery Potential 1035 V, 1.5 Megohm and Gap were in Series.

With this theoretical background, the report will now proceed to studies of emission of rf radiation from discharge gaps in the range of .0005 inch to .010 inch. It will be shown that rf radiation from electrical discharges in this gap range yield the same type of discharge from electronic components where gaps on the order of thousands of wave lengths of light exist. Radiation from a number of malfunctioning components will also be presented.

Section 3

EXPERIMENTAL

INTRODUCTION

When research is undertaken which covers a wide range of frequencies of electromagnetic radiation (rf radiation), difficulties are certain to be encountered. This is especially true when the range included .15 to 400 megacycles per sec. Whenever an electrical apparatus operates and brush discharges are present, rf radiation is emitted. For example, a short wave radio receiver can detect rf radiation emitted from a vacuum sweeper which has a commutator and contacting brushes. Very definite peaks may be tuned in. Around an electronic laboratory with malfunctioning devices, a background of electrical noise exists and the presence of peaks may be discovered.

Initially, the work was done in a screen room. In order to use the vacuum system to make preliminary studies of brush discharges in different gases, the experimental apparatus was moved from the screen room into the laboratory. It was found the rf radiation emanating from the gap was more intense than most background noises and could be easily differentiated from them. It could easily be differentiated for example from radio stations encountered. Most of the work was done outside the screen room under these conditions. From this experience, however, it has been found that it would be highly desirable to work in a shielded room made of solid metal making sure the number of open holes in the walls are a minimum. Higher sensitivity of the receiving instruments could be employed.

As work progressed, the technique in using the instruments and reliability of measurements improved. The data, therefore, became more meaningful. A number of experiments were performed on different phases of the approach. Some of the experiments to be presented are somewhat exploratory in nature and will suggest further areas of concentrated research in which present knowledge and techniques can be employed. A number of the experiments will present a greater understanding of the discharge mechanism and its application to malfunctioning electronic systems.

19

INSTRUMENTATION

For the study of emitted rf radiation, four instruments are employed.

1. The noise analyzer, Singer Co., Empire Model NF 105.
2. The spectrum analyzer, Singer Co., Model SPA-4a.
3. The receiver, Hallicrafter, Model SX62A.
4. The oscilloscope, Tektronix 581-A.

For other instruments used, see Appendix A.

The performance of these instruments have been studied with a signal generator and the instruments have been employed in experimental work. Their eccentricities and potential uses are established. The technique for making accurate, reliable, and reproducible rf radiation measurements also has been accomplished. Applications of the technique to measurements will be presented for a number of experiments.

The Instruments for Radio Frequency Radiation Measurements

The NF 105 noise analyzer has been found to be a good instrument for making measurements of rf radiation frequencies and their amplitudes. The frequency range with two plug-in units is .15 to 200 Mc/sec. Peak frequencies can be determined or complete frequency curves can be plotted using the db meter on the instrument to measure amplitudes and detect peaks.

The SPA-4a spectrum analyzer is useful in making fast, visible measurements of peak frequencies over the entire spectrum. The complete frequency spectrum is made visible by turning a knob. The 10 cm scale can be made to represent a range of 5 Mc/sec or 70 Mc/sec for a given frequency setting on the dial. The complete scale is swept 60 times a second. The instrument measures voltage at the input as a function of the frequency of the source. A radio station would be represented by a spike with a width Δf. Thus, each spike will represent energy over a frequency range of Δf. These spikes will hereafter be designated as energy bands. The Δf range is dependent on the sweep rate of the instrument which, in this case, is kept constant at 60 sweeps of the scale per second. This instrument is similar to a spectroscope in which the slit width

represents Δf, and the thermopile reading represents its energy. Photographs can be made of regions of the rf spectrum and thus integrate the energy bands from a pulse source of energy. For a high pulse rate discharge, peaks become apparent because of the large number of energy bands. The instrument measures frequencies from 10 to 400 Mc/sec on one scale, on another, 350 to 1000 Mc/sec.

The frequency response of the radio receiver is far from linear. It responds from .550 to 108 Mc/sec. It finds its greatest use in continuously monitoring the brush discharge. The character of the discharge can be determined by the sound produced on the receiver and frequencies can be quickly checked.

A Tektronix oscilloscope 581-A with a rise time of 5.4 nanoseconds is being used to study the rf radiation output of the electrical discharge and the output of a photomultiplier, the cathode of which receives light from the electrical discharge. The effect of various circuit components in the discharge and receiving circuits can be determined. The rise time of this instrument is marginal.

A Radio Frequency Measuring Technique

In order to study the effect of various parameters of the electrical discharge and determine its mechanism, it is required that accurate, reliable, and reproducible measurements be made. The following technique for measuring frequencies has been developed after trying several others. Use is made of the method employed for measuring spectrographic plates and x-ray diffraction films. Information from both plates and film is obtained by measuring line position and line density. This technique is applied to the noise analyzer. The general idea is to measure the peak height above the background noise. This can be easily done on a plotted curve of decibel readings vs frequency. However, peak-frequency data for the entire spectrum from .15 to 400 Mc/sec can be recorded in a relatively short time without plotting a curve, as will be seen later.

The input to the noise spectrometer may be an antenna consisting of a 4-inch equilateral triangle of copper screen wire with a small copper wire soldered perpendicular to its mid-point. The wire fits into the female connection on the 30-foot cable made to match the instrument. This antenna and connecting cable has sufficient signal pick-up for the small electrical discharge employed in

21

these experiments. The cable itself, when attached to the noise analyzer, has been tested with a signal generator. No oscillations were found and the response curve is essentially linear for this signal. The antenna-cable combination has been giving satisfactory pick-up for signals over the entire frequency range with no obvious difficulties. The effect of the cable on peak frequencies will be discussed further on in the report.

The output of the noise analyzer is detected with both earphones and the output meter which reads from -6 to 20 decibels. The two readouts are most convenient. The signal from the electrical discharge is usually a high energy signal which can be distinctly heard on the earphones. It can be clearly distinguished from radio stations, and other noises which are received and sometimes interfere. Even if the peak frequency of electrical discharge is only a few tenths of a megacycle from an interference, the peak frequency can be detected and its amplitude estimated with the earphones and db-meter combination.

In order to pick up both weak and strong signals, the signal is sought when the intermediate frequency (i.f.) gain of the instrument was in the range of 12 db to 20 db. The earphone signal level was adjusted for comfortable hearing. Thus, for example, a frequency can be found at 22 Mc/sec. It can be tuned in using both earphones and db-meter. When possible, the i.f. gain is then turned up so that the meter reads 20 db for the peak. The background is then sought on either side of the peak. This is the point where the earphones and/or the meter indicates the lowest reading. This number is subtracted from the peak reading; the difference is the estimated strength or amplitude of signal. As frequencies progress in magnitude, they become weaker so that the i.f. gain must be increased and, in fact, the 20 db reading cannot be attained without changing the db sensitivity of the instrument. In this case, the background reading is always taken close to the peak and the peak amplitude is taken as the difference of the peak reading and the background reading. This procedure gives results from which frequencies and their estimated amplitude can be compared.

SOME APPLICATIONS OF THE FREQUENCY-AMPLITUDE MEASURING TECHNIQUE

The data to be discussed were taken in room air for clean nickel electrodes .050 inch diameter polished flat on 4-0 metallographic

paper and wiped clean with lint free paper. The gap, g, was set
at .004 inch. The power supply circuit for the gap is shown in
Figure 9. The power supply was set at 1500 volts dc, the potential
across the gap was about 600 volts dc. By-pass capacitors to give
low impedance to the fast rise time electrical brush discharges (nano-
seconds) may be seen across resistors as well as line filters which
pass only 60 cycles. The gap is indicated along with the three rece-
iving antennas. The antennas may be moved to various positions with
respect to the discharge. The major portion of the power supply
was housed in a copper screen box surrounded by a solid copper
box fabricated from 0.022 inch thick copper. This precaution limited
rf radiation to the electrical discharge circuit outside of the box.
The purpose was to limit radiation as nearly as possible to electrical
discharge itself. The following frequency-peak amplitude data were
taken on the noise analyzer from .15 to 200 Mc/sec. It was extended
with data from spectrum analyzer to 400 Mc/sec. That these
frequencies were present at the time of measurement has been
verified by the signal in the earphones and turning the electrical
discharge off and on. The detail results are shown in Appendix A,
SRL Report 552-4. A resume of the principal results follows.

With this experimental set-up, 25 peaks were found over
the range of 6.4 to 310 Mc/sec. Cables of 30-foot and 13 foot lengths
were most effective in changing the number and frequency of the
peaks. Data for the 13-foot RG 8/U cable indicated the addition of
four peaks and the absence of 8 peaks from the peaks found for the
30 foot cable. The effect of the removal of the by-pass capacitors
for the resistors was negligible. Distances of the antennas from the
gap of 12 inches and 48 inches had little effect on the peaks except
to reduce the number by a few because of the larger distance. Both
of these distances were in the far field position; no standing waves
were found effective in the measurements. Using a battery, a 100
megohm current limiting resistor and the gap for the rf generating
system, five peaks were missing and one was added. Since it is
known that the electrical discharge changes to modes, it is not con-
sidered a constant source of spectral radiation. Therefore, the change
of a few in the number of frequencies is not too significant. These
results indicate the type of power supply had very little significance
on the number of peaks. The simplification of the receiver circuit
will be discussed later. It was found from peak data taken under the
same experimental conditions at different intervals during the ex-
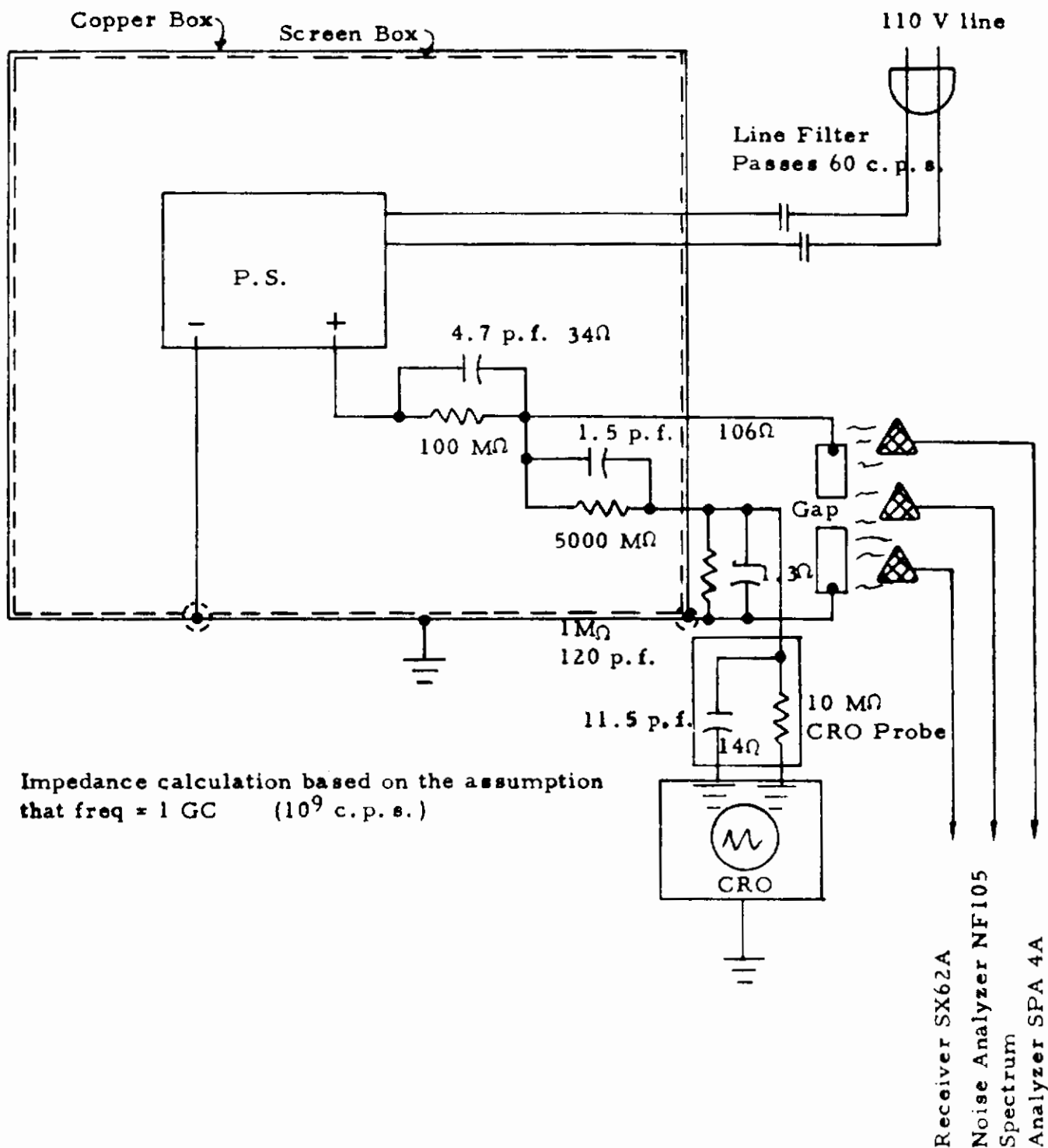periments that peak frequencies could be measured to better than 2%

23

Figure 9. A Power Supply Studied for the Generation of RF Radiation from an Electrical Discharge in Air at a Pressure of 718 Torr.

and 4% of the frequency measured. During these experiments, the electrical discharge was not changed so that its effect on peak frequencies was not discussed.

A COMPARATIVE STUDY OF THE PULSED RADIO FREQUENCY AND VISIBLE RADIATION EMITTED FROM A HIGH TENSION DISCHARGE IN AIR

Earlier discussions indicated that temporary discrete pulses of rf radiation arise from active discharge circuits of the type being studied. The pulse repetition frequency (prf) depends in a complicated way upon many factors. Among other factors are the inductance, capacitance, and resistance of the discharge circuit, the physical arrangement of the circuit components, the discharge gap separation and configuration, the pressure of the gas in the discharge gap and the type of gas. Typical prf values for circuits of the types employed in the present studies (for typical circuits, see below) ranged from a few per second to several hundred thousand per second.

Pulse repetition frequencies of the order of $(10)^2$ pulses per second ordinarily were employed in order to obtain moderate discharges. Direct visual observation of the light pulses emitted from the discharge at such repetition frequencies in general yield little quantitative information since the eye will integrate the light from the closely spaced pulses, each of short duration.

In order to determine what correlation exists between the occurrence of the pulses of rf radiation and the pulses of light emitted from the discharge, preliminary study of the relationship between the two was undertaken. The correlation between the voltage pulse in the discharge circuit and the light pulses was also investigated.

Measurement of the light pulses was accomplished as follows. Light emitted from the discharge gap was directed upon the photoemissive surface (S-20) of an electron photomultiplier vacuum tube. This was satisfactorily achieved by optical coupling of light from the gap through a 2-inch diameter convex lens (8-inch focal length) and thence, upon the surface of the photomultiplier. The output of the photomultiplier was fed onto one input of a dual beam cathode

ray oscilloscope through a co-axial cable.

The principal elements of the experimental arrangement are shown in Figure 10.

The rf pulses were detected by using a triangular screen wire antenna (see Figure 23, E and F for antenna detail), the output of which was fed by co-axial cable to the second input of the dual beam cathode ray oscilloscope. In an alternate experiment, the voltage pulse developed across a 100 kΩ resistor placed in series with the discharge gap was fed into this second input of the cathode ray oscilloscope. Thus, that voltage pulse could be compared with the pulse output of the photomultiplier. A schematic of the appropriate elements of this experimental arrangement is shown in Figure 11.

In Figure 12 is shown a typical oscillogram as displayed on the cathode ray oscilloscope for the case where the input number 1 was fed from the photomultiplier and input number 2 was fed from the screen wire rf antenna pickup. The inputs were displayed simultaneously at identical sweepspeeds.

The different slopes obtained for the two traces was caused by differences in the circuits employed to couple the two signals into the cathode ray oscilloscope. The significant feature of the oscillogram presentation is that there is a 1:1 correspondence indicated between the prf of the light pulses and the rf pulses emitted from the discharge circuit. Results which were essentially identical to those presented above were obtained for the case where the voltage pulse developed across the 100 kΩ resistor was substituted for the rf antenna output on the cathode ray oscilloscope input number 2.

The presence of extensive ringing in the receiver circuits prevented analysis of the detail of the voltage pulse under high resolution. The presence of ringing is due in large measure to receiver circuit and cable capacitance, inductance and resistance. Even if the ringing was absent, an analysis of the true voltage pulse from the discharge would be difficult if not impossible for the present case. This is because the rise time of the cathode ray oscilloscope is of the same order as the length of the voltage pulses which are being measured. Thus, the true pulse form is displayed convolved with the instrument limited rise and decay curve of the cathode ray oscilloscope.

26
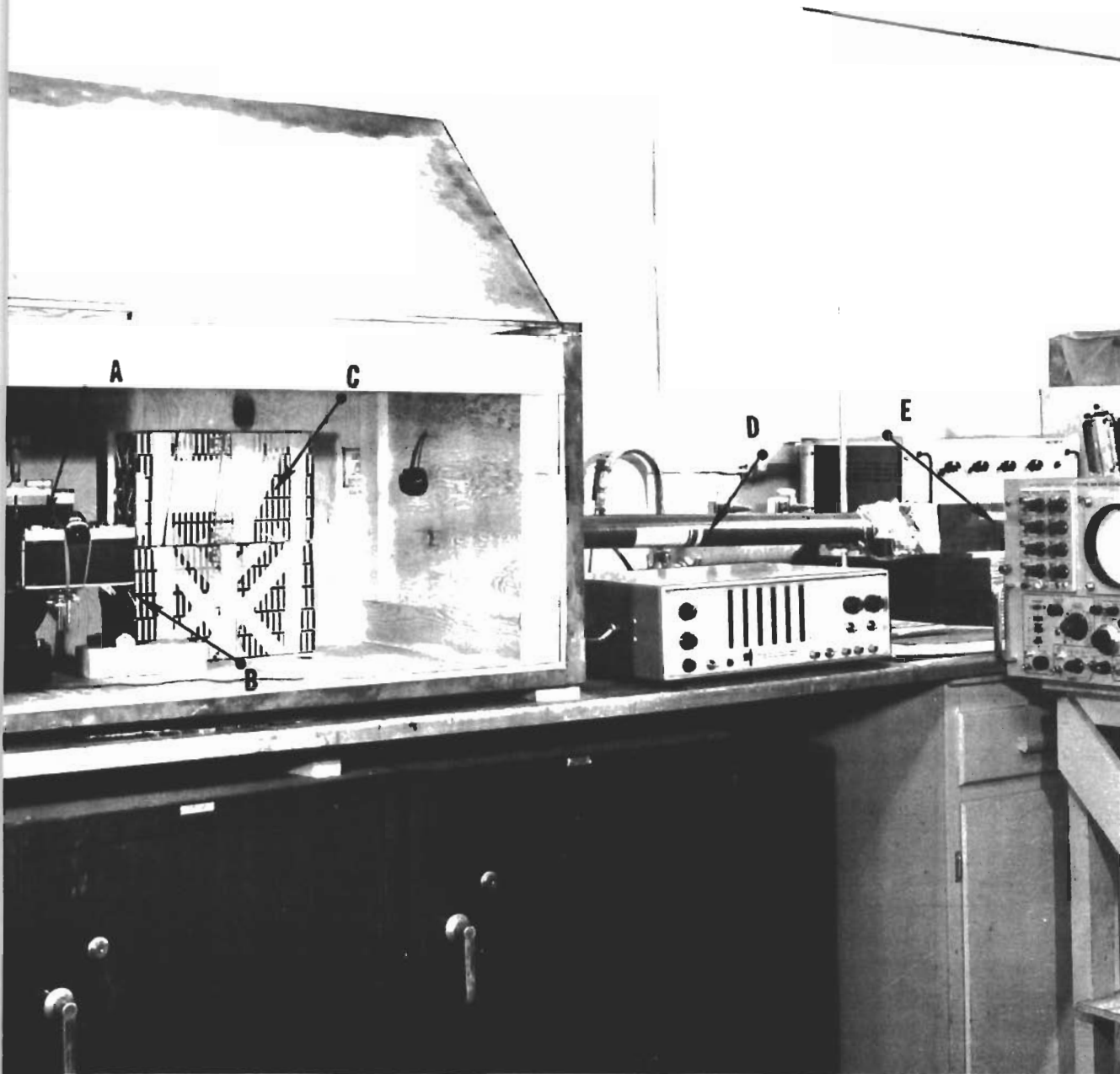
A. Discharge Gap (see Figure 22)
B. Convex Lens
C. Battery Power Supply for the Discharge
D. Light Shield
E. Electron Photomultiplier Vacuum Tube and Enclosure

Figure 10. Photomultiplier Apparatus

27
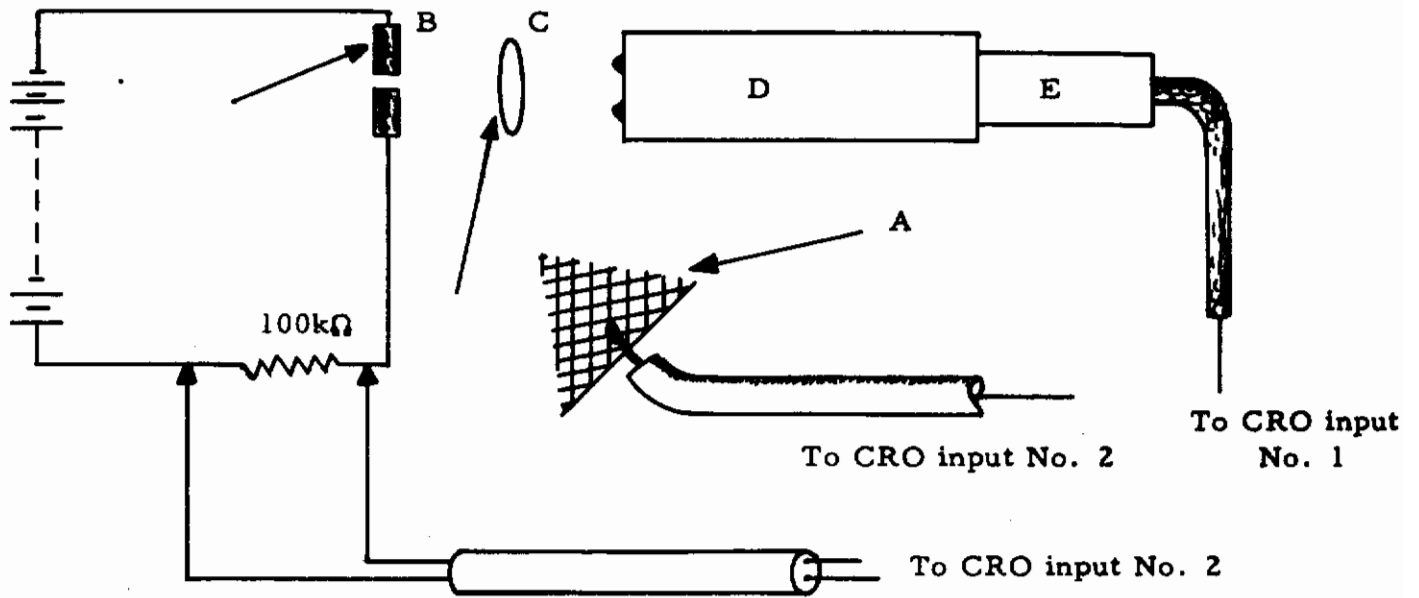
A - Screen Wire Antenna (Rf antenna)

B - Discharge Gap (Ni electrodes, .050 in. dia.) Separation .005 in.

C - Lens

D - Light Shield Tube

E - Photomultiplier

Figure 11. Pulse Studies Apparatus
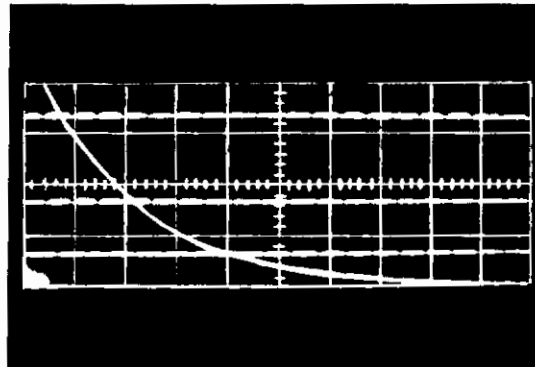
Upper Trace: Photomultiplier Output
Horizontal Units - $2(10)^{-4}$ sec/cm

Lower Trace: RF Antenna Output
Horizontal Units - $2(10)^{-4}$ sec/cm

Figure 12. Typical Discharge Pulses

INSTRUMENTATION INVESTIGATIONS

Receiver Circuits

The Cathode Ray Oscilloscope: The cathode ray oscilloscope is used extensively in the present studies to display voltage pulses of short duration. Correct interpretation of the pulse forms displayed on the cathode ray oscilloscope requires an understanding of those factors related to the oscilloscope and detection equipment which can effect significant changes in the form of the display presented.

Experiments were performed to demonstrate the effect of receiver circuit parameters upon the signal display. A discharge circuit, as shown in Figure 11, was employed as a source of pulsed rf radiation. The receiver consisted in this instance of a triangular screen wire antenna (3-inches on each side), a co-axial cable to conduct the voltage pulse developed at the antenna to a display device, and a cathode ray oscilloscope (Tektronix 581A) as the display device. The rf source-to-antenna spacing was 26 inches. The variable parameter in the first experiment was the length of the cable connecting the antenna to the cathode ray oscilloscope, and in the second, it was the cathode ray oscilloscope. A typical set of cathode ray oscilloscope trace patterns obtained under these conditions are shown in Figure 13. Cables A, B, and C, respectively, were a 30-inch, a 81-inch, and a 27-inch length of co-axial cable (RG 58C/U). The dependence of the ringing frequency and amplitude upon the different cable lengths and different oscilloscopes employed is clear upon examination of the traces shown in Figure 13. Future experiments must be designed so as to minimize the amount of ringing. This ringing apparently arises entirely within the receiving circuitry.

Spectrum Analyzer (SPA-4a) and Noise Analyzer (NF-105): A series of experiments were performed using two spectrum analyzer devices. One device was the SPA-4a spectrum analyzer, and the other was the NF-105 noise analyzer. The source of rf for the first series of experiments was a discharge from a circuit of the type shown in Figure 11. The rf source was located 12 feet from the receiver equipment and the antennas. The variable parameters were the antennas, the cables coupling the antennas to the receivers, and the receivers themselves. Antenna of various lengths (1 inch to 9 feet), a variety of physical configurations ("long-wire," dipole,

30

Oscilloscope 581A

| Cable A | Cable B | Cable C |

.01 μsec/cm, .2 v/cm   .01 μsec/cm, .2 v/cm   .01 μsec/cm, .2 v/cm
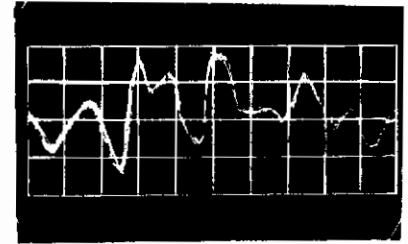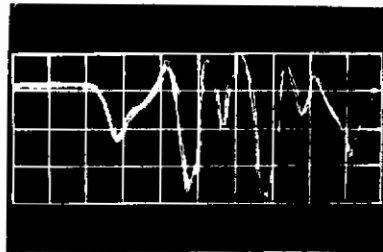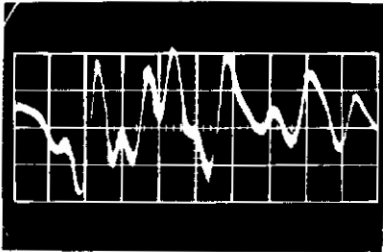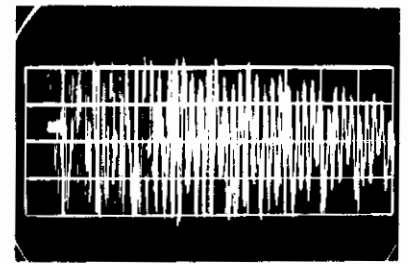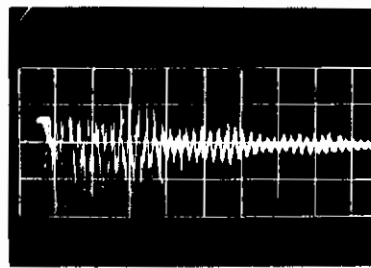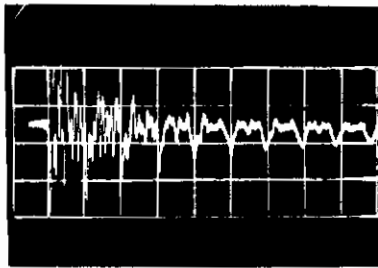
.05 μsec/cm, .2 v/cm   0.1 μsec/cm, .2 v/cm   .10 μsec/cm, .1 v/cm

Oscilloscope 532
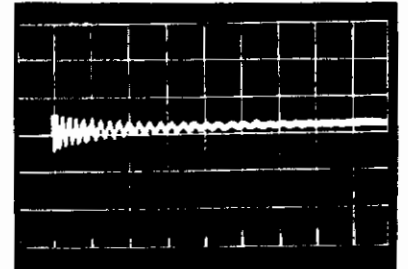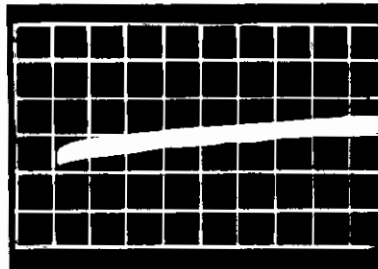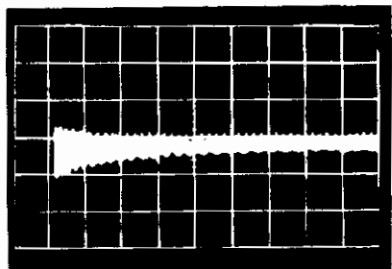
.2 μsec/cm, .05 v/cm   .2 μsec/cm, .05 v/cm   .2 μsec/cm, .05 v/cm

Figure 13. Oscilloscope Traces Showing the Effect of Different Lengths of RG 58 c/w Cable on the Ringing Frequency of a Pulse Discharge. Cable A, 30 Inches Long; Cable B, 81 Inches, Cable C, 27 Inches.

31

and folded dipole) and various orientations with respect to the recei-
ver-source system were employed. The existence of peaks in the
rf spectrum, and their relative amplitudes were found to depend
strongly upon all of the above stated variables.

In another experiment, all experimental parameters were
held fixed except the receiver devices. Using different receivers,
different peaks were detected. Correlation between the peaks ob-
tained using two different receivers was exceedingly low. A typical
set of data obtained by interchanging receivers upon a given antenna
system is shown in Table 2. A triangular screen wire antenna
was employed (3 inches on each side).

Table 2

Radio Frequency Peak Spectrum from Two Receivers	
SPA-4a (Spectrum Analyzer) frequency in Mc/sec	NF-105 (Noise Analyzer) frequency in Mc/sec
25.8	12.5
28.5	29.0
38.4	39.0
42.0	57.5
49.0	64.5
52.3	85.0
57.0	91.0
66.0	99.0
77.0	170.
92.5	225.
102.	275.
109.	308.
131.	430.
184.	
198.	

32

It should be noted that with sufficient receiver "gain" or transmitter amplitude rf radiation was detected over the entire spectrum scanned (10 to 200 Mc/sec for the NF-105 and 10 to 430 Mc/sec for the SPA-4a).

It may be stated on the basis of the above described studies that the nature of the peak structure in the rf emission spectrum arising from a discharge circuit is highly dependent upon the receiver and signal coupling system employed. Further, the nature of the cathode ray oscilloscope display presented for an rf voltage pulse from the discharge circuit is found to depend upon the cathode ray oscilloscope, antenna, cables and other circuitry employed in the reception and display of the signal.

For a comparison of the frequency distribution of the rf emitted from a gap discharge circuit with that of another "continuous" distribution rf source, the output of an impulse type noise generator was employed. Such a device is contained within the NF-105 case and its output, when coupled directly into the input of the NF-105, is essentially flat as measured by that device. It is a "typical" noise generator spectrum.

If the coupling of the noise generator to the NF-105 is made through an extended co-axial cable instead of direct coupling, peaks in the noise spectrum are observed. If the output of the noise generator is coupled by one antenna to another antenna which feeds in the NF-105 input, then very strong peaking of the spectrum is observed. Different antennas yielded different peak distributions. The series of experiments outlined in the discussion of the cathode ray oscilloscope and analyzer investigations were performed using as a source of rf radiation the output of the noise generator. This latter sequence of studies yielded results quite similar to those obtained from the gap discharge rf radiation studies described earlier. The similarity was particularly good considering the fact that the antennas and coupling systems for the two sources were not identical.

Radio Frequency Source

A series of experiments were performed in which circuit parameters of the discharge circuit were varied and the effect of these variations upon the rf spectral peaks was noted. The instruments

33

used to detect the rf radiation were the SPA-4a and the NF-105.
The distance from the discharge circuit to the receiver was held
nearly constant at 6 feet throughout this series of experiments.
Figure 14 shows the various circuit arrangements employed for
the discharge circuit in this series of studies.

Various combinations of component values were employed
in each circuit. The applied voltage E was varied from 412 to 2060
volts in each circuit. Furthermore, the entire sequence was duplicated
using a rectified dc power supply as a source.

Based on the results of the above studies, the following
conclusions were reached:

i)   The only instance where an appreciable change of the
     rf spectral peak distribution could be induced by changes
     of a discharge circuit parameter was for the case of a
     capacitor across the power supply terminals.

ii) The pulse repetition frequency changes as the circuit
     parameters are altered.

iii) The amplitude of the rf remains relatively constant
     as the circuit parameters are varied over a wide range
     of values.

iv) Variation of the supply voltage altered the pulse repetition
     frequency but not the rf emission spectrum.

v)   Rectified, filtered dc yields the same results as pure dc

vi) The spatial orientation of the discharge circuit with
     respect to the receiver circuit has no effect upon the
     frequency distribution of the rf spectrum for reasonable
     source antenna to receiver antenna separation distances.

vii) Altering the antenna system of the source appears to
     have little if any effect on the frequency distribution of
     the rf radiation emitted. The amplitude of the rf signal
     does, however, change.

34
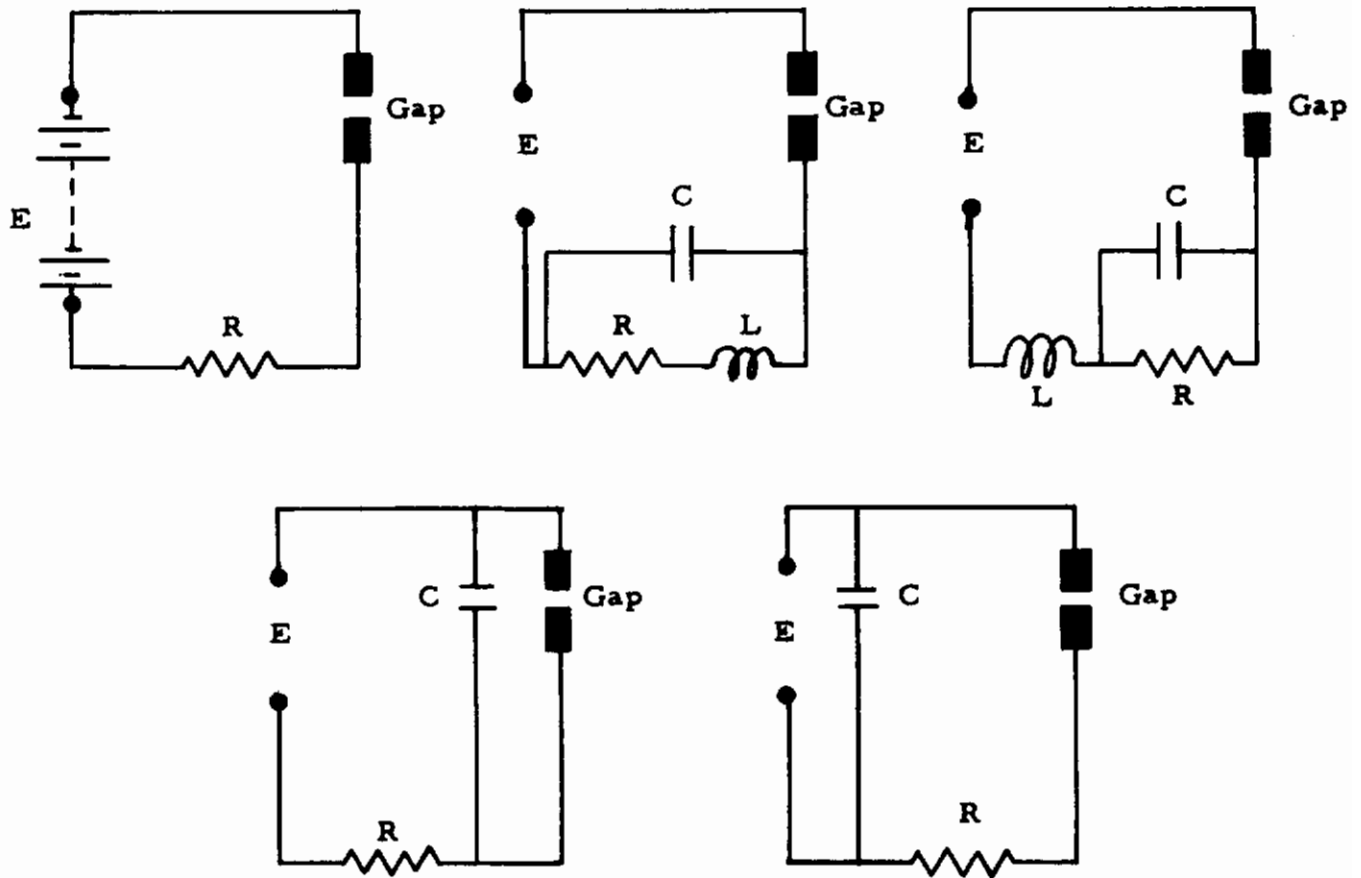
The range of values of the circuit parameters employed in these circuits were as follows:

$$R = 100K \text{ to } 4.7M$$

$$C = 600 \,\mu\mu f \text{ to } 6000 \,\mu\mu f$$

$$L = 10 \,\mu h \text{ to } 300 \,\mu h$$

Figure 14.   Discharge Circuit Diagrams

35

Preliminary investigations of the influence of pressure and the type of gas employed in the discharge gap indicated the following may be true:

i) The rf spectral distribution does not appear to be significantly affected by changes in the pressure of the gas in the gap of 716 to 200 torr.

ii) The rf spectral distribution appears to be markedly influenced by the type of gas present in the discharge gap.

EXPERIMENTAL PROCEDURE

A typical experiment will be described which indicates data that has been obtained from a small gap of copper electrodes in laboratory air at atmospheric pressure.

The electrodes consist of high purity copper wire .050 inch in diameter with the ends squared and finally polished with 4-0 metallographic paper. They were cleaned in an acid solution, washed in distilled water, and rinsed in alcohol to assure the elimination of surface contaminants. The electrodes were supported inside of the bell jar of a vacuum system by a mechanical device which permits adjusting the electrode gap from a few tenths of a mil to .5 inch or greater as required, see Figure 15. In this experiment, the copper electrodes were separated .001 inch (.00254 cm) in an atmosphere of dry oil-free air at a pressure of 730 torr. Since in previous experiments, the brush discharge was found to be the type of discharge emitting rf radiation, the experiment begins by gradually raising the voltage of the dc power supply to the region just below the initiation potential of the first discharge.

Electromagnetic radiation may be detected through space or by a change in magnetic flux near the B+ wire of the power supply.

The following are important observations which will ultimately aid in the explanation of the mechanism of the discharge and the rf radiation characteristics:

When the voltage is carefully increased, a single pulse can be produced. The pulse rate can be increased or decreased depending upon whether the voltage applied to the electrical discharge is raised or lowered.

36
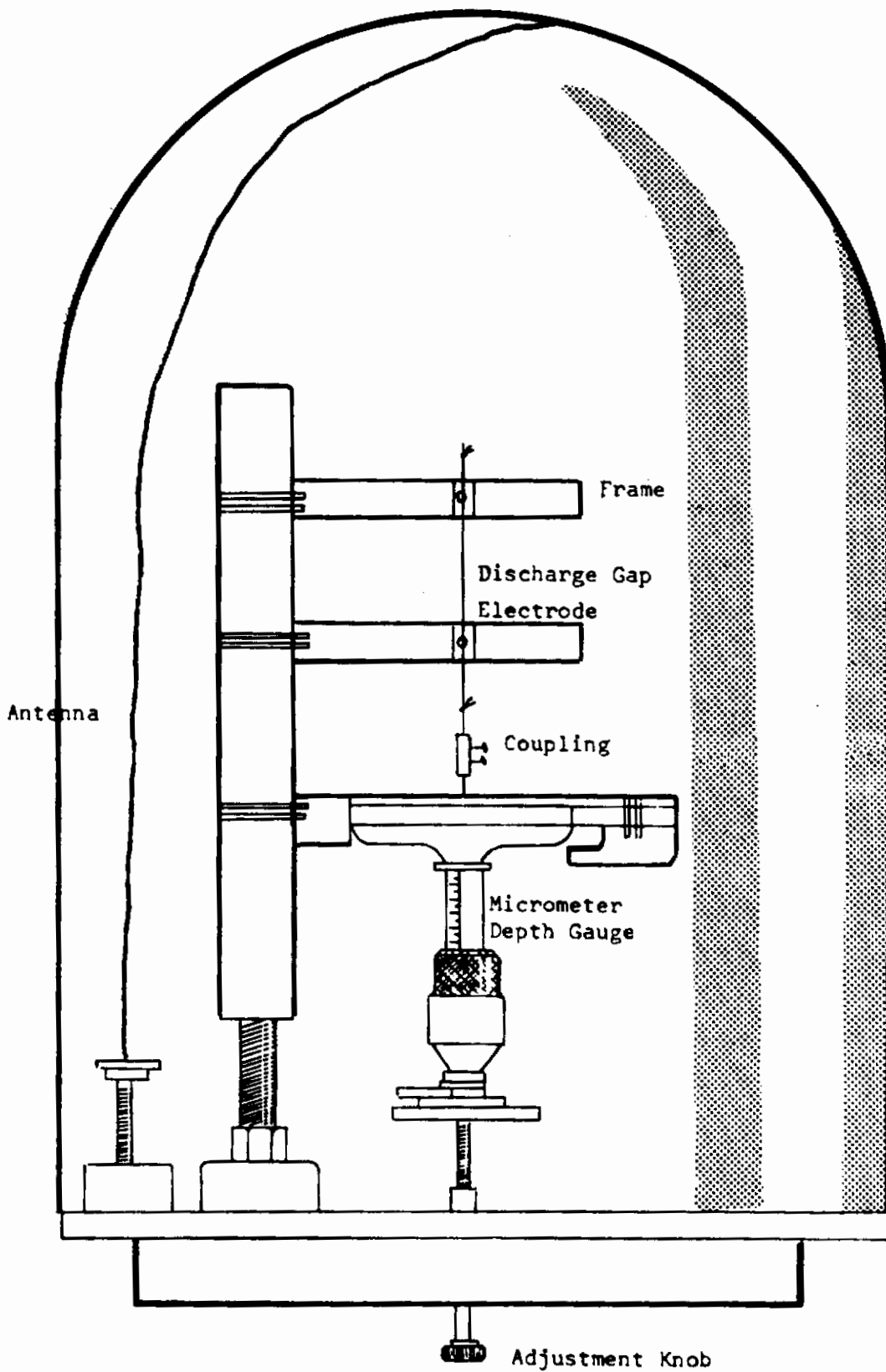
Figure 15. Experimental Set-up in the Vacuum Chamber

There is output from the rf receiver's audio detector during each pulse, over the entire range of 550 kc/sec to 108 Mc/sec, which is the range of the receiver.

With the spectrum analyzer set on 0-5 Mc/sec sweep width, (2.5 Mc/sec on either side of the center frequency setting), energy bands can be observed for frequencies of 10 to 400 Mc/sec.

As observed on a spectrum analyzer, the general background of the rf emissions is a relatively constant amplitude, random distribution, white noise. Superimposed upon this background, throughout the spectrum, are areas which display a minority of higher amplitude energy band emissions which, when integrated photographically over a period of time, would describe the envelope of the rf spectrum of the emissions.

EFFECTS OF APPLIED VOLTAGES ABOVE THE THRESHOLD FOR PRODUCING PULSES

As the voltage applied to the electrodes of the discharge is increased, the reoccurrence rate of the electrical discharge increases sufficiently so that the envelope of the energy bands appear above the background level. This is observed on a spectrum analyzer, Figure 5. As the applied voltage is increased, the pulse rate increases and more peaks become visible above the background level. A spectral peak or envelope is represented as a group of energy bands which form a maximum above the background level. The number of these peaks increase substantially for potentials above an applied potential of 1500 volts dc used in this experiment.

The electrical circuit for the above experimental work is shown in Figure 6. It consists essentially of two parts, the electrical discharge circuit, and four types of signal receivers. The bell jar of the vacuum system to control the gas and pressure environment around the gap is not shown.

The Electrical Discharge

The electrical discharge circuit consists of the dc power supply, a current limiting resistor (40 to 500 MΩ are currently being used), discharge electrodes, an electrometer voltmeter and 121 kΩ resistor as a voltage divider for the oscilloscope and counter instru-

38

ments. The electrode gap can be varied from tenths of mils to wider gaps. Very little difficulty with particulate contamination is experienced at the low current levels being used.

The Signal Pickup

The four instruments being used as signal receivers are a Singer Metrics spectrum analyzer, an oscilloscope, a counter, and a short-wave radio receiver, see Figure 16 and Appendix B. The peaks detected on the receivers are shown in the right hand part of Table 3. In order not to clutter this part of the table with a repetition of peaks, only peaks and estimated amplitudes are given at selected voltages.

Data

The data were obtained from a brush type of electrical discharge described above. As the power supply voltage, V_{ps}, was increased, see Column 1, Table 3, the current in the circuit was increased. The current is calculated from the power supply voltage, the voltage across the gap, and the measured resistance in the circuit. Column 3 shows discharges from a few hundredths of a microampere to 44 microamperes. The current-vs-power-supply voltage is plotted in Figure 17. Attention is called to the fact that this current is not sinusiodal nor is it a steady current as is that current coming from an arc discharge which occurs at higher voltage. The current is made up of a series of integral discharges which increase numerically with applied voltage, Column 6. The current calculation depends upon the dc voltage measurement of the electrometer voltmeter which is possible above the average or rms value for the circuit. Column 2 shows small variation of the voltage across the discharge gap, V_g. It varies from 655 volts at zero discharge current to 475 volts at 44.2 microamperes.

CALCULATIONS AND DISCUSSION

The field, E, Column 4, is the ratio of the gap voltage, V_g, and the gap spacing, i.e.

$$E = \frac{Vo}{d} \left(\frac{Volts}{cm} \right).$$

It varies from 258,000 to 183,000 volts/cm. The voltage across the gap decreases with the current in the circuit, and thus the field
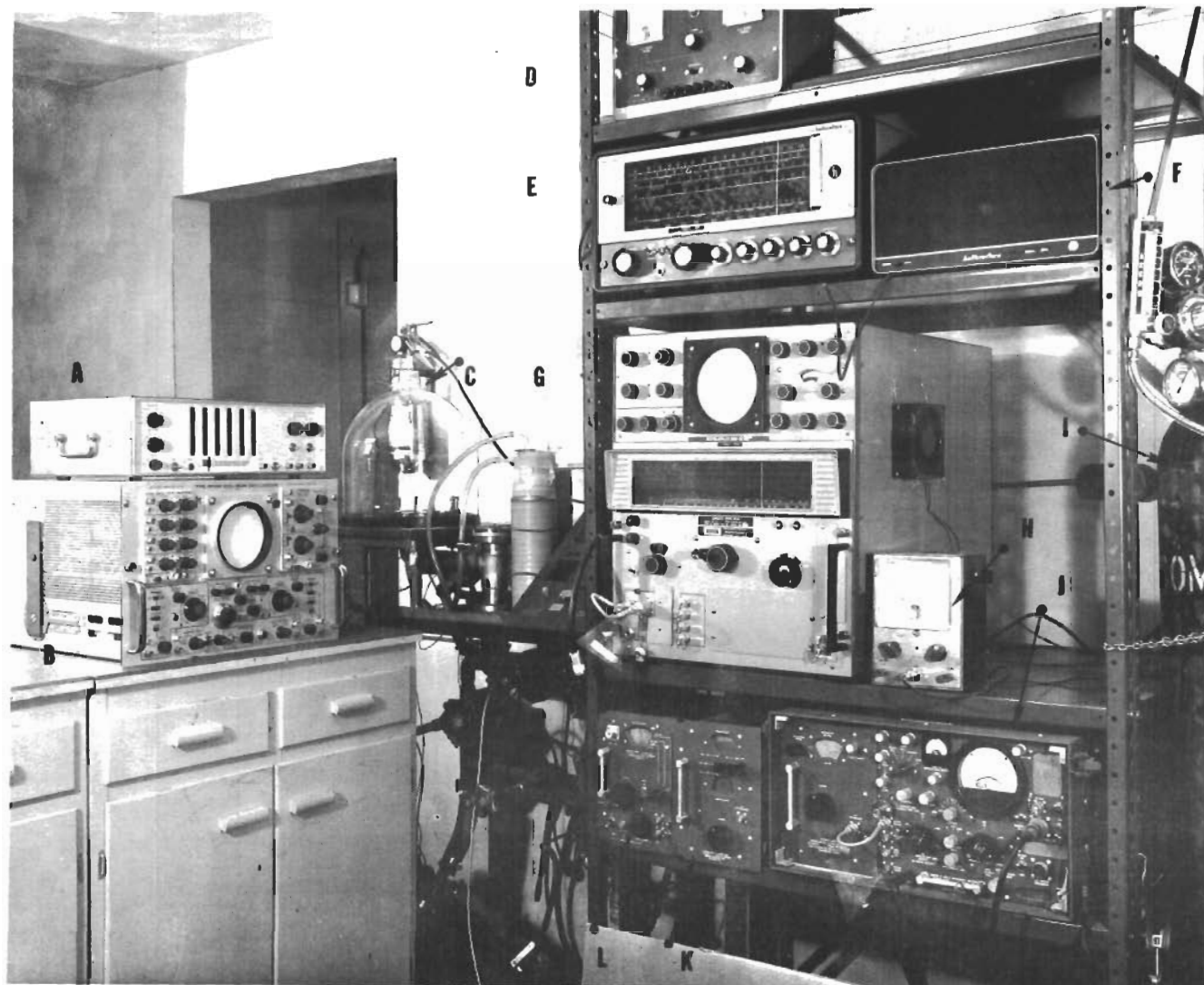
Figure 16. Essential Apparatus for Studying RF Radiation from Brush
Discharges. A - Electronic Counter; B - Type RM565 Dual Beam
Tektronix Oscilloscope; C - Vacuum Bell Jar; D - Heathkit DC Power
Supply; E - Hallicrafter Model SX62A Receiver; F - Speaker; G - Singer
Spectrum Analyzer Model SPA-4a; H - RCA, AC VTVM; I - Argon
Tank; J - Singer Noise Analyzer Model NF105 with 20-200 Mcps
Plug-in Unit; K - Plug-in Unit .15-30 Mcps; L - Plug-in Unit 14-150 Kcps

Table 3

Data on the Brush Type Electrical Discharge between Copper Electrodes in Clean, Dry, Oil-free Air
Wire Diameter 050", Gap = 001" (.00254 cm), Pressure 730 torr

V_{ps} Power Supply (Volts) (1)	V_G Gap (Volts) (2)	i Circuit Current (Microamps) (3)	E field (Volts/cm) (4)	E/p $\left(\dfrac{Volts}{cm\ torr}\right)$ (5)	Counts Per Sec. (6)	Electrons Per Count (7)	$\alpha^{(1)}$ $\dfrac{Electrons}{cm}$ (8)	$1/\alpha^{(2)}$ $\dfrac{cm}{Electrons}$ (9)	Peaks Appearing on the Spectrum Analyzer Frequency (estimated amplitudes) (mcps) (10)
655	655	0	$258 \times 10^{+3}$	363	.417		3900	2.56×10^{-4}	Discrete frequencies began to appear on spectrum analyzer
660	658	025	259	355	4				
670	668	025	263	360	4	1.2×10^{11}	3800	2.64×10^{-4}	Discrete frequencies over range of frequencies, 550 Kcps - 400 mcps
680	665	.188	262	359	8				21 High amplitude at 20 - discrete frequencies over entire frequency range
690	675	.188	266	365	11	2.74×10^{11}	3940	2.54×10^{-4}	21 Discrete frequencies over range of instruments - high amplitude at 21 mcps
700	660	.500	260	366	25				21 Discrete frequencies at all frequencies - high at 21 mcps
710	665	.563	262	359	125	$.73 \times 10^{11}$	3800	2.64×10^{-4}	21 34 48
720	545	2.19	214	294	200				
730	555	2.19	218	299	250				
740	545	2.44	214	294	260				
750	558	2.40	220	302	265	1.45×10^{11}	3210	3.12×10^{-4}	21(9.5) 34(5) 48(4) 53(5) 103(3) 130(4) 75(2)
760	550	2.63	216	296	300				
770	540	2.87	212	290	330				
780	540	3.00	212	290	340				
790	535	3.17	210	288	370				
800	532	3.35	209	286	375				
850	518	4.15	204	280	450				
900	508	4.90	200	274	550				
950	500	5.63	197	270	650				
1000	495	6.40	195	267	680	1.51×10^{11}	2780	3.60×10^{-4}	21(10) 34(10) 48(4) 54(4.5) 105(3)
1100	494	7.58	194	265	855				
1400	482	11.46	190	260	1250				
1600	475	14.05	187	256	1500				
1800	475	16.55	187	256	1800				
2000	475	19.01	187	256	2040				
2500	470	25.4	185	254	2825	1.445×10^{11}	2550	3.92×10^{-4}	21(10) - 31(3.5) 34(9) 38(3.5) 44(4) 49(3) 54(5) 105(3) -
3000	475	31.8	187	256	3700				
4000	475	44.2	187	256	4200				21(11) 24(3) 31(4) 34(11) 36(6) 44(4) 49(5) 54(6) 105(3.5) 140(2)
					Avg	1.50×10^{11}			

(1) α = ion pairs produced/cm of path by an electron

(2) $1/\alpha$ average distance traversed by an electron to produce an ion pair

41

decreases. One of the most important parameters of an electrical discharge is $\dfrac{E}{p}$ $\left(\dfrac{\text{Volts}}{\text{cm torr}}\right)$. This parameter is the electric field E divided by the pressure, torr (or mm of Hg). This parameter uniquely describes the discharge and is utilized for comparing different discharges and for using data of similar work on file in books and publications. The values of E/p between 363 to 256 $\left(\dfrac{\text{Volt}}{\text{cm torr}}\right)$ in this experiment are relatively high and apply to small gaps representative of discontinuities in electronic components. At lower pressures and wider gaps and higher currents, lower E/p values are representative. The percent of electron energy loss by various types of impacts may be determined with E/p, reference 13 loc. cit. P. 725. For the values of E/p obtained in this experiments, ionization by direct impact of the electron with the atoms is indicated.

Inasmuch as the circuit current was made up of small discharges, an electronic counter was placed in the circuit, Figure 6, to count them, Column 6 of Table 3. This Column gives the number of counts per second and should be proportional to the current. Figure 18 shows a plot of counts per second or electrical discharges per second against power supply voltage. A comparison of Figure 18 with Figure 17, current-vs-power-supply voltage, shows good agreement. The exact cause for the sharp break in this curve between 710 and 720 volt dc power supply voltage has not been determined. It may be caused by a change in the nature of electrode surfaces, oxidation for example, though it appears this should take place at high voltages.

It is now possible to calculate the average number of electrons per count, Column 7. This is accomplished by converting the current in Column 3 into electrons per second and dividing it by counts per second. Though in the beginning, the electrons per count are somewhat random, it appears that after the discharge becomes more stable, the electrons per count remains constant at 1.50×10^{11}. This is based on the loading current in the circuit and is not the transient current of the discharge.

The Avalanche

With the present data, it appears reasonable to regard each electrical pulse of the discharge as an avalanche buildup. Each
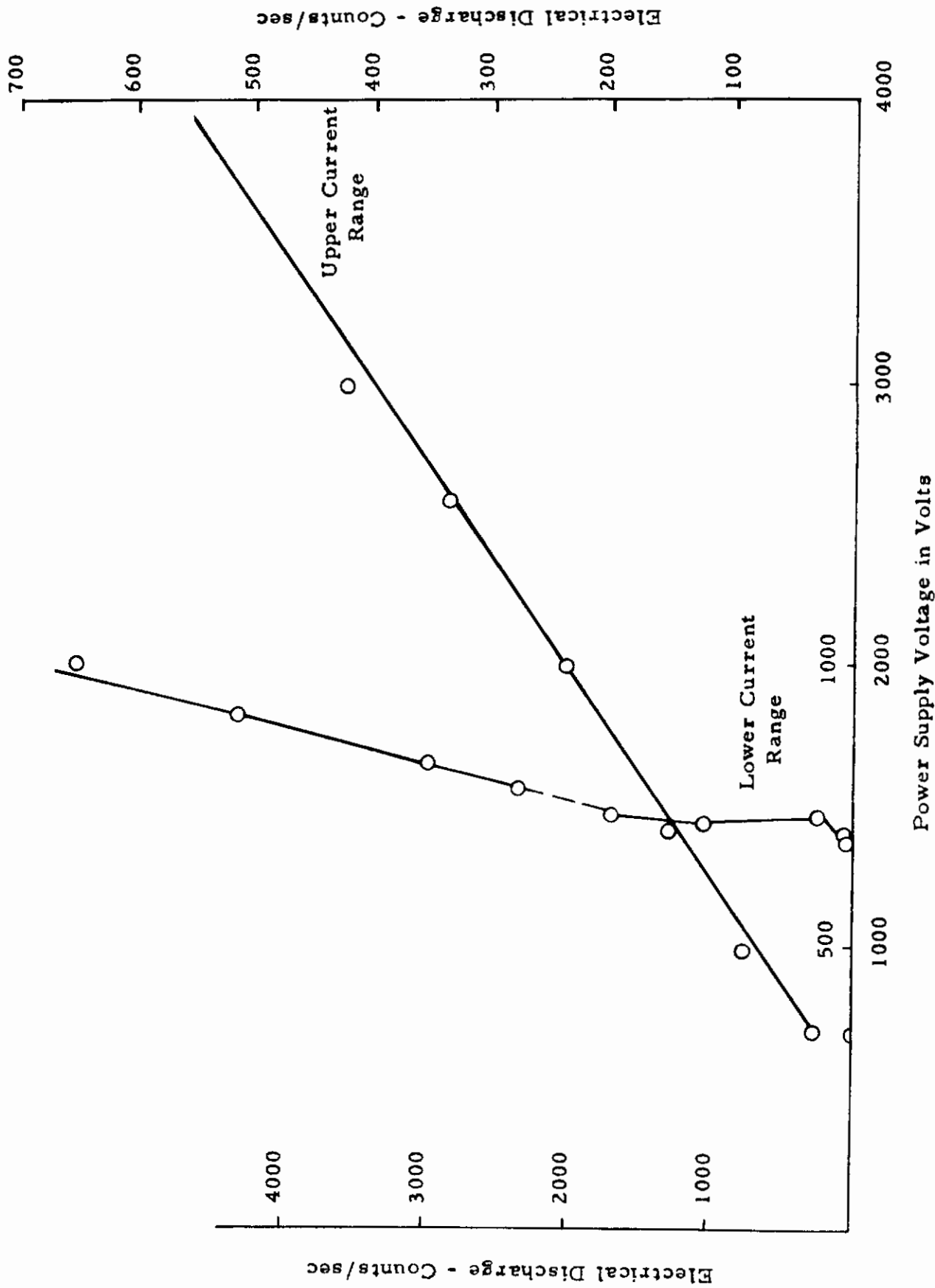
43

Figure 18. Electrical Discharges - Counts/sec VS Power
Supply Potential for a Brush Discharge Between Copper Electrodes
Systems Research Labs   JWB   14 Oct. 64

avalanche gives rise to energy bands as detected on spectrum analyzer instrument. Column 7, electrons per pulse, is not interpreted as the number of electrons per avalanche. The avalanche itself is a transient phenomenon and must be treated as such in determining its characteristics.

Townsend's First Coefficient: From the parameter $\frac{E}{p}$ a very important coefficient can be found. This is known as Townsend's first coefficient, α (alpha). It is defined as the number of positive ion and electron pairs produced by an electron when traveling one centimeter in the direction of the field. Values of α/p are obtained from a curve of α/p vs E/p[14]. When α/p is multiplied by p, the atmospheric pressure, 730 torr, the coefficient α is obtained. The units of α are $\frac{electrons}{cm\ path}$ or $\frac{+\ ions}{cm\ path}$. According to Loeb, reference 13 loc. cit. P. 651, $\frac{1}{\alpha}$ represents the average distance an electron traverses to make a new ion pair, that is, the ionizing free path. The data given in Column 9 for $\frac{1}{\alpha}$ is the ionizing free path for the experiment. It is not the mean free path which for air is 6.77×10^{-6} cm at 730 torr and $20^\circ C$[15].

The last column in Table 3 indicates the presence of peak frequencies. A greater number of peak frequencies become observable as the discharge rate increases. It will be noted the number of peaks increase from one to eleven and the current also increases. Thus, more electrons participate; energy bands become numerous and more peaks become visible on the spectrum analyzer. The energy bands in the background also increase. It is interesting to note the relation between the number of free paths, $\frac{1}{\alpha}$, which occur within the gap distance, d.

Free Path $\left(\dfrac{d}{1/\alpha} \right)$	Number of Peaks	
9.6	3	before equilbrium
8.2	7	
7.1	6	
6.5	9	
Average 7.2	7.3	

It appears that the number of peaks are approximately equal to the number of free paths within the gap. This result occurred in two additional experiments. It is thus tempting to conclude that each avalanche is terminated at the end of each free path due to a space charge effect, that the number of peaks are a function of a number of free paths, and that the peak energy would be a function of the position within the gap. However, present experimental data and photo-micrographs will not permit these conclusions.

Numerous exploratory calculations have been made. These data are related to energies and velocities of electrons, to ionization potentials of pertinent gases and atomic copper. The threshold field is related to the work function of three different metal electrodes.

1) The energy of an electron traveling the free path λ depends on the field: energy $= Ee\lambda$. Values taken from the horizontal row Table 3 at 750 volts dc power supply voltage yields

$$\underline{68.8 \text{ eV}} \text{ over this path.}$$

This energy lies between the III and IV ionization potentials of oxygen and nitrogen; that is, between 47 and 77 eV.

2) The terminal velocity over a free path using the kinetic energy equation is $V = 4.82 \times 10^8 \dfrac{cm}{sec}$.

3) Threshold voltages were obtained for various gap widths The threshold voltage is the lowest voltage at which a single discharge occurs. This is not an accurate experiment because the lowest voltage depends upon the state of ionization of the gas and the patience of the experimenter to wait for the discharge to occur. Threshold voltages were obtained and plotted against gap separation for 1/4-inch diameter aluminum electrodes in air at atmospheric pressure of 730 torr. From the slope of the curve the field $E = 59 \times 10^3 \dfrac{Volts}{cm}$

$$\frac{E}{p} = 80.9 \frac{Volts}{cm \text{ torr}}$$

46

$$\frac{\alpha}{p} = .42$$

$$\alpha = 306 \ \frac{electrons}{cm}$$

$$\lambda = \frac{1}{\alpha} = 3.27 \times 10^{-3} \ cm, \ ionizing \ free \ path$$

$$Ee\lambda = \ energy \ of \ electron \ at \ end \ of \ free \ path,$$
$$3.10 \times 10^{-10} \ ergs = 194 \ eV$$

4) From Table 3, calculations were made with data obtained from the horizontal row beginning with $V_{ps} = 750$ volts dc

a) $E/p = 302 \ \dfrac{Volts}{cm \ torr}$

b) $P = 730$ torr

c) $pd = 1.864$ torr, cm

d) $\alpha = 3210 \ \dfrac{electrons}{cm}$

e) $1/\alpha = 3.12 \times 10^{-4} \ \dfrac{cm}{electron}$

f) $\dfrac{d/1}{\alpha} = 8.15$ paths in gap

g) $n = 1e^{\alpha d} = e^{3210 \times 2.54 \times 10^{-3}} = e^{8.15} = 3463 \ \dfrac{electron}{cc}$

providing electron avalanche traveled across the gap

h) $n = 1e^{3210 \times 3.12 \times 10^{-4}} = 2.7 \ \dfrac{electrons}{cc}$ at end of first free path

5) Calculations of transient effects from oscillogram, Figure 19 and photomicrograph, Figure 8.

a) Peak volts = 12.5
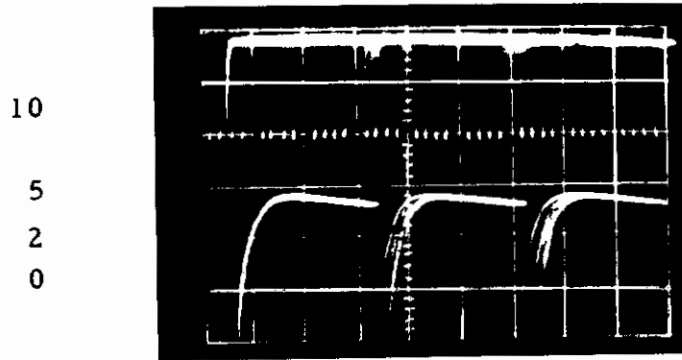
(a)

Volts/cm; see calibration, 2 milliseconds/cm

V_{max} = 12.5 volts, V_{avg} = 2.06 volts calculated
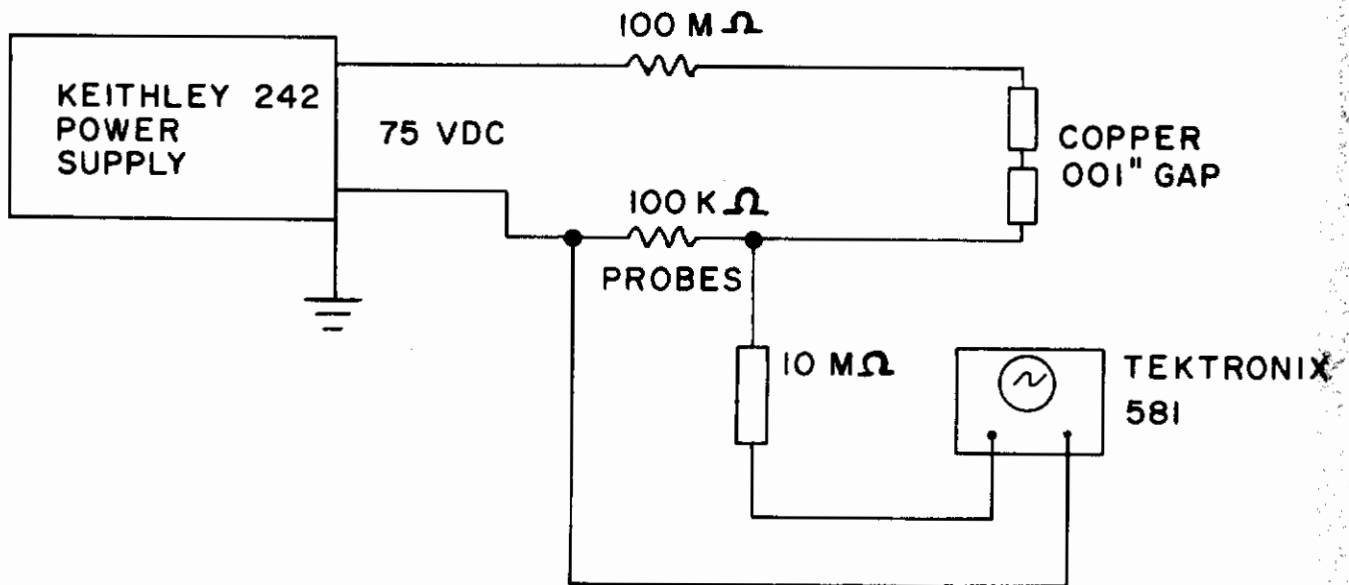
(b)

Figure 19. Oscilloscope Picture Used in Calculation of Electrical Parameters of Transient Phenomena in an Electrical Pulse Discharge, (a) Picture, (b) Circuit. Figure 8 also Employed.

b) Average volts = 2.06

c) Time base at which 2.06 volts occurred = 7.1 milliseconds Oscilloscope probes across 100 kΩ

d) Current = 2.06 x 10^{-5} amperes

e) 3.30 x 10^{14} $\frac{\text{electrons}}{\text{sec}}$, current equivalent

f) Estimated rise time from oscilloscope trace, Figure 19a = 6.5 x 10^{-9} sec (approximately)

g) Electrons generated per pulse 3.30 x 10^{14} x 6.5 x 10^{-9} = 2.14 x 10^{6} electrons

h) Volume of discharge, Figure 8 = 2.84 x 10^{-5} cm^3

i) Electron density n = $\frac{2.14 \times 10^{6} \text{ electrons}}{2.84 \times 10^{-5} \text{ cm}^3}$ =

7.55 x 10^{10} $\frac{\text{electrons}}{cm^3}$

j) Consider the pulse as the generation of an avalanche, $n_o = 1$
from $n = n_o e^{\alpha d}$, 7.55 x $10^{10} = 1 e^{\alpha 2.89 \times 10^{-2}}$,
d = 2.89 x 10^{-2} cm where d was measured from Figure 9c at a magnification of 220X, α is calculated to be 870 $\frac{\text{electrons}}{\text{cm}}$

k) A free path $\lambda = \frac{1}{\alpha} = $ 1.15 x 10^{-3} $\frac{\text{cm}}{\text{electron}}$

l) Number of free paths in the gap $= \frac{d}{1/\alpha} = \frac{2.89 \times 10^{-2}}{1.15 \times 10^{-3}}$ = 25.1. The maximum number of peaks measured for nickel electrodes was 25.

m) Assuming the discharge is a plasma like discharge, the frequency, ν, for an electron density of

49

$7.55 \times 10^{10} \dfrac{\text{electrons}}{\text{cm}^3}$ paragraph 5i above, $\nu =$

$8.98 \quad 7.55 \times 10^{11}$ (16)   from which $\nu = 2.46$ Mc/sec. This frequency occurs within the range of peak frequencies measured, though it is low.

n) p x d $\sim$ mass of gas between electrodes.   pd = 730 torr x 2.89×10^{-2} = 21.1 torr cm

o) $\dfrac{\alpha}{p} = \dfrac{870}{730} = 1.19 \dfrac{\text{electrons}}{\text{cm torr}}$

p) $\dfrac{E}{p} = 130 \dfrac{\text{Volts}}{\text{cm torr}}$ P5-168 reference 16

q) $E = 730 \times 130 = 95,000 \dfrac{\text{Volts}}{\text{cm}}$,   the field from transient calculations

r) E_c the field across the gap from circuit parameters

$E_c = \dfrac{1667 \quad \text{Volts}}{2.89 \times 10^{-2} \text{ cm}} = 57,700 \dfrac{V}{\text{cm}}$

s) $E - E_c = 95000 \dfrac{V}{\text{cm}} - 57,700 \dfrac{V}{\text{cm}} = 37,300 \dfrac{V}{\text{cm}}$

This increase in field, $33,700 \dfrac{V}{\text{cm}}$, can possibly be due to the positive ion movement toward the cathode which forms a positive ion sheath near the cathode. This effectively decreases the gap distance between the positive electrode and the cathode and thus, increases the field.

These calculations and numerical data can be used as a reference to understand what is occurring in the brush type discharge for small gaps at atmospheric pressure. The data also aid in comparing the present work with that performed by others in which different experimental parameters were used. These data will be used in later discussions.

BRUSH DISCHARGE DATA FOR GOLD, COPPER AND ALUMINUM ELECTRODES

The object of this experiment was to obtain data from brush discharges under constant $\dfrac{E}{p} \dfrac{\text{Volts}}{\text{cm torr}}$ for different electrode materials.

50

This would permit the determination of Townsend's first coefficient α, the free path $1/\alpha$, the approximate energy per free path, and the final velocity per free path. The field E (volts/cm) could also be compared with the work function of the electrode material.

Three electrode materials with the following characteristics were employed:

	Wire Diameter (inch)	Purity (%)	Preparation
Gold	.050	99.99	Polished flat with 4-0
Copper	.050	Commerical Grade	metallographic paper and wiped clean with lint free paper
Aluminum	.032	99.7	
Nickel	.050	99.9+	

Experimental procedure consisted of determining the threshold voltage across six gap separations .001 inch, .002 inch, .004 inch, .006 inch, .008 inch and .010 inch. By threshold voltage, it is meant that voltage producing a field, which when applied very slowly, produces a single electrical pulse discharge, or avalanche across the electrodes. The circuit consisted of a dc voltage regulated power supply, and a current limiting resistor of 100 megohms in series with the gap. A Kiethley instrument was used to measure the voltage across the gap. The discharge occurred in dry, oil-free air. A representative plot of threshold voltage against gap separation is shown in Figure 20. The slope of this curve gives the field, E (Volt/cm). The calculated data are shown in Table 1. Since the calculated data are field dependent, the table shows how they vary with electrode materials. Of particular interest is the free path, $1/\alpha$, and the number of free paths per gap. It will be noted in these experiments that the free path $\lambda = 1/\alpha$ is constant for a given electrode material. It is also to be noted that the number of free paths increases with gap separation. The latter are shown in the last section of the Table. The maximum number of free paths is about 9 in a 10 mil gap.

The curve in Figure 21 shows the proportionality which exists between the threshold field emission and the work function of the metal electrodes.
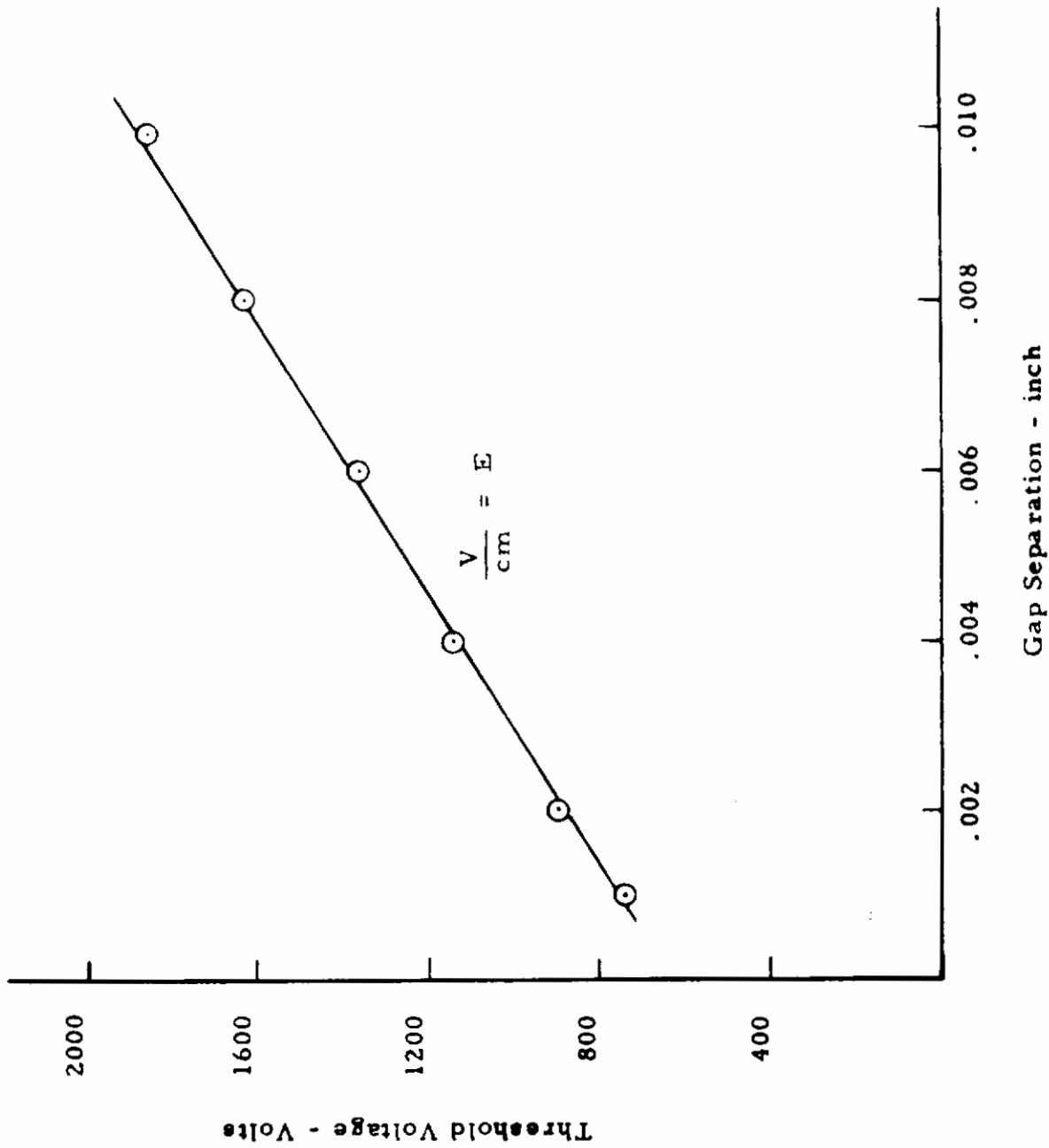
Figure 20. Threshold Voltage VS Gap Separation
Aluminum Electrodes, 032 Inch Dia.
Flat Polished Faces
Systems Research Labs, Inc.   JWB   16 Oct. 1964

TABLE 4

Data showing threshold fields for electron emission from the cathode of a brush discharge for three metals plus their work functions and other data, discharge in dry, oil-free air.

	E Volts/cm	$\dfrac{E}{p}$	$\dfrac{\alpha}{p}$	α	$\lambda = \dfrac{1}{\alpha}$	K.E. (ev)
Gold	63.2×10^3	87	.48	346	2.89×10^{-3}	183
Copper	56.4×10^3	78.4	.32	231	4.33	244
Aluminum	48.4×10^3	67.8	.21	152	6.58	318

(continued)

	v (cm/sec)	Work function θ (ev)
Gold	8.04×10^8	4.82
Copper	9.25	4.46
Aluminum	16.0	4.08

E = field; p = 721 torr; α = electrons, + ions produced per centimeter of path by an electron; λ = free path for an electron; K.E. = terminal electron energy after it moves across a free path λ; v = terminal electron velocity assuming uniform field, no collisions, etc.

Gap Separation		Number of free paths in the gap for Pressure=721 torr for dry, oil-free air		
Inch	cm	Gold	Copper	Aluminum
001	2.54×10^{-3}	.88	.59	.39
002	5.08	1.41	.94	.62
004	10.16	3.52	2.34	1.55
006	15.24	5.27	3.52	2.32
008	20.32	7.02	4.7	3.10
010	25.4	8.8	5.9	3.86

Electrode diameter: Gold 050 inch; Copper 050 inch; Aluminum 032 inch; Polished Flat with 4-0 metallographic paper.
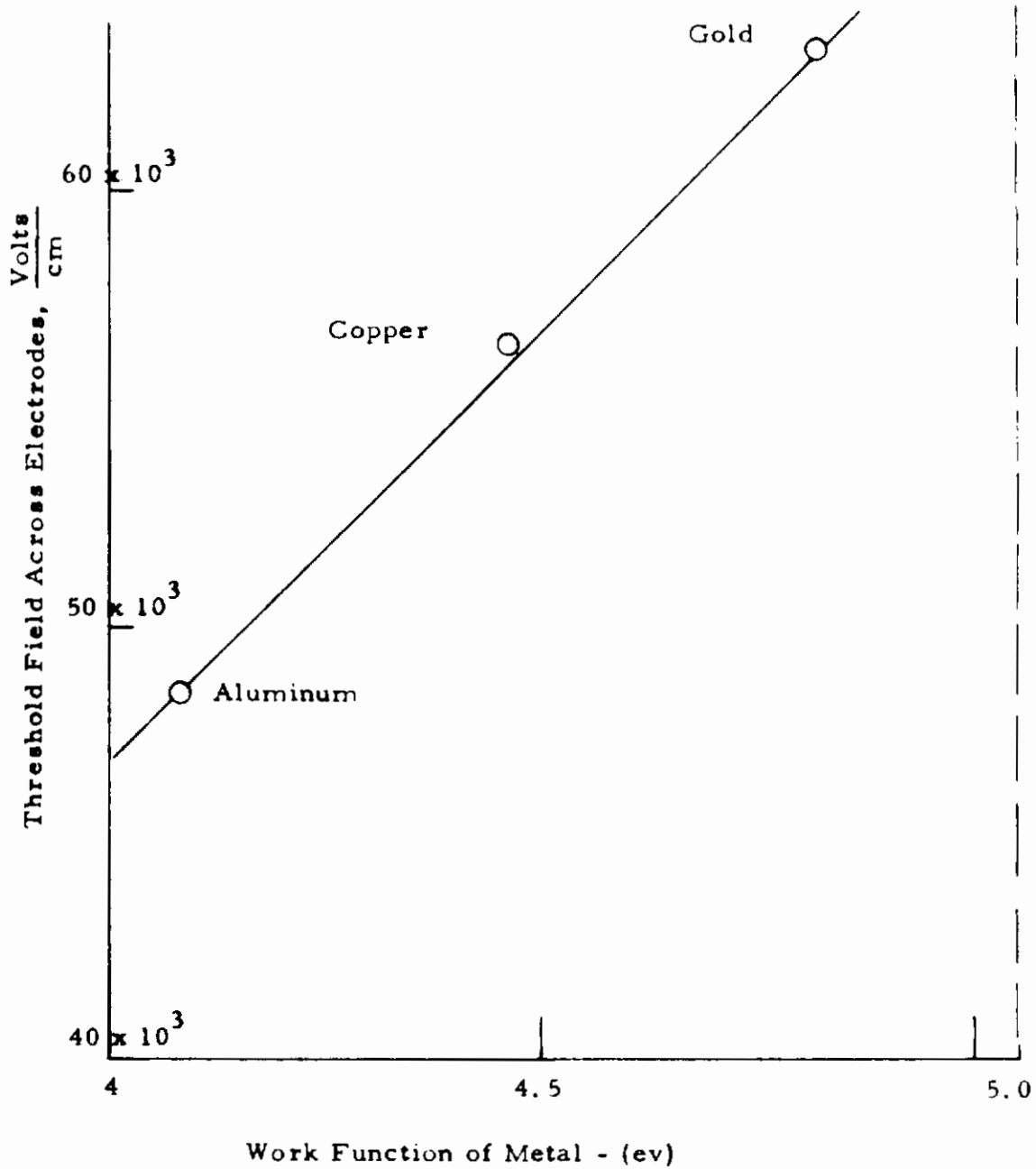
Figure 21. Threshold Field for Electron Emission from Cathode of Electrical Discharge Against Work Function of Three Metals
Systems Research Labs, Inc.   JWB   17 Dec. 1964

The effect of residual electrons, negative ions and positive ions on the ejection of the electron from the cathode by the field is minimized by the waiting period between discharges and increasing the potential slowly. It may be seen from Figure 20, that the potential required to form an avalanche is a linear function of gap between the electrodes. This curve also indicates by its slope the field to eject an electron from the flat surface of the electrode.

Field emission is the vibration of electrons from a solid by a strong electric field at the surface. The value of the field has been obtained for threshold emission for three metals. The electronic work function is the energy needed to remove an electron from the Fermi level in a metal to a point an infinite distance from the surface of the metal. If the energy required by the field to extract the electron from the surface is equal to the work function, the distance S the electron moves can be determined. The following equation was utilized:

$$EeS = \text{Work Function, where} \quad \begin{array}{l} E = \text{threshold field} \\ e = \text{charge on electron} \\ S = \text{distance traveled} \\ W.\ F.\ \text{Found in Published Tables} \end{array}$$

The data and results are shown in the following table:

Table 5

Distance Electron Moves During Field Emission				
Metal	Threshold Field	Distance of Field Reaction	Diameter of Atom	
	$E \dfrac{\text{Volts}}{\text{cm}}$	S(cm)	D(cm)	$\dfrac{S}{D}$
Gold	63.2×10^3	7.6×10^{-5}	2.878×10^{-8}	2.64×10^3
Copper	56.4×10^3	7.9×10^{-5}	2.55×10^{-8}	3.1×10^3
Aluminum	48.4×10^3	8.5×10^{-5}	2.82×10^{-8}	3.01×10^3
			Avg.	2.9×10^3

These data indicate that field emission forces react over a distance

55

of approximately 8×10^{-5} cms and when the electron attains this distance it is free of forces of the atom. Another way of stating the results is the following: When the electron is about 3000 atomic diameters away from the atom it is free from atomic influence. The field then takes over and accelerates the electron in the gas which produces an avalanche.

Section 4

APPLICATION OF RESULTS OF RADIO FREQUENCY RADIATION STUDIES TO MALFUNCTIONING ELECTRONIC COMPONENTS AND CIRCUITRY

It now becomes desirable to relate the techniques and results of studies of brush discharges discussed above to malfunctioning electronic components. The studies above involved gaps from .0005 inch to .010 inch requiring $\pm$ 500 volts across the gap. However, numerous electronic components and circuitry operate at much lower voltages and thus, much smaller gaps. The transition from small to very small gaps can best be made by describing the experiment with a cold solder joint. Before doing this, however, two experimental devices must be discussed.

GAP MEASUREMENT APPARATUS

It had been found in the studies above that the gap could be adjusted with a single micrometer with a least measurement of .001 inch, Figure 22. The gap could be adjusted for maximum rf output, that is, the maximum number of electrical pulses per second.

Very Small Gap Adjustments

For low voltage gaps, it is very difficult to adjust the gap for a continuous brush discharge. A lever 16-1/8 inches long attached to the micrometer was employed to move the micrometer. It was found the movement of the end of the lever to cover the complete range of the gap discharge for the cold solder experiment was 5/8 inch. A second micrometer was therefore employed at the end of the lever arm to facilitate adjusting the very small gap. Figure 23 shows the gap micrometer caliper B, the lever C and the second micrometer D which adjusts the lever. A movement of .001 inch on the lever micrometer caliper D will cause a gap separation of 63×10^{-8} cm or 63 Angstroms. A lever movement of 5/8 inch indicates the discharge range for the solder gap to be about 4000 Angstroms. The absolute measurement of the gap spacing was not made for two reasons. First, a fiducial mark had not been established and second, the apparatus was not firmly mounted to merit accurate measurements of this magnitude. However, sufficiently close estimates can be made to guide interpretation of the data.

57
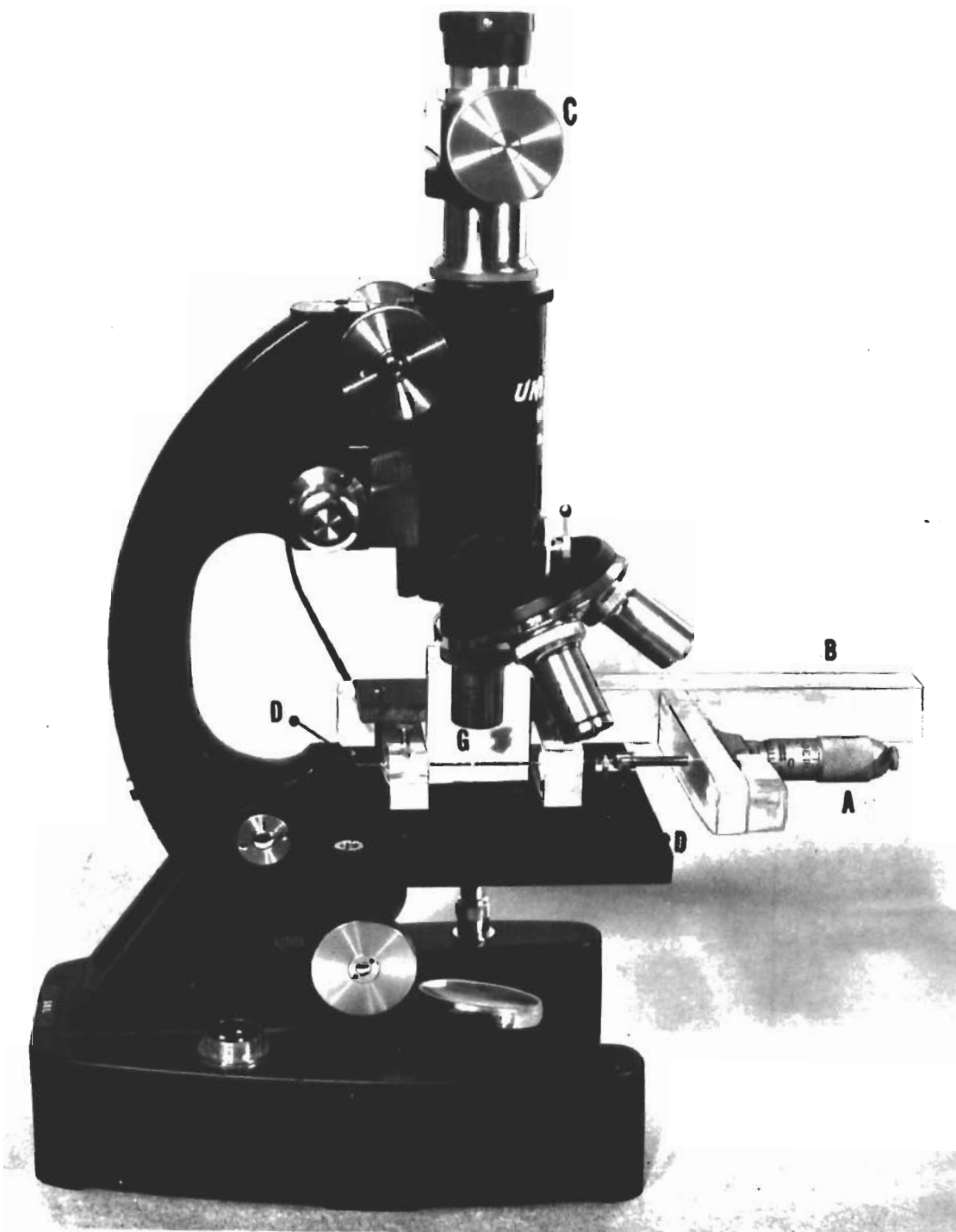
Figure 22. Monocular Microscope with Vertical Illuminator with Electrode Supports Attached. A - Micrometer Depth Gauge .001 Inch; B - Polystyrene Support; C - Filar Eye Piece; D - Contact Junction for Minigator Clips.

58
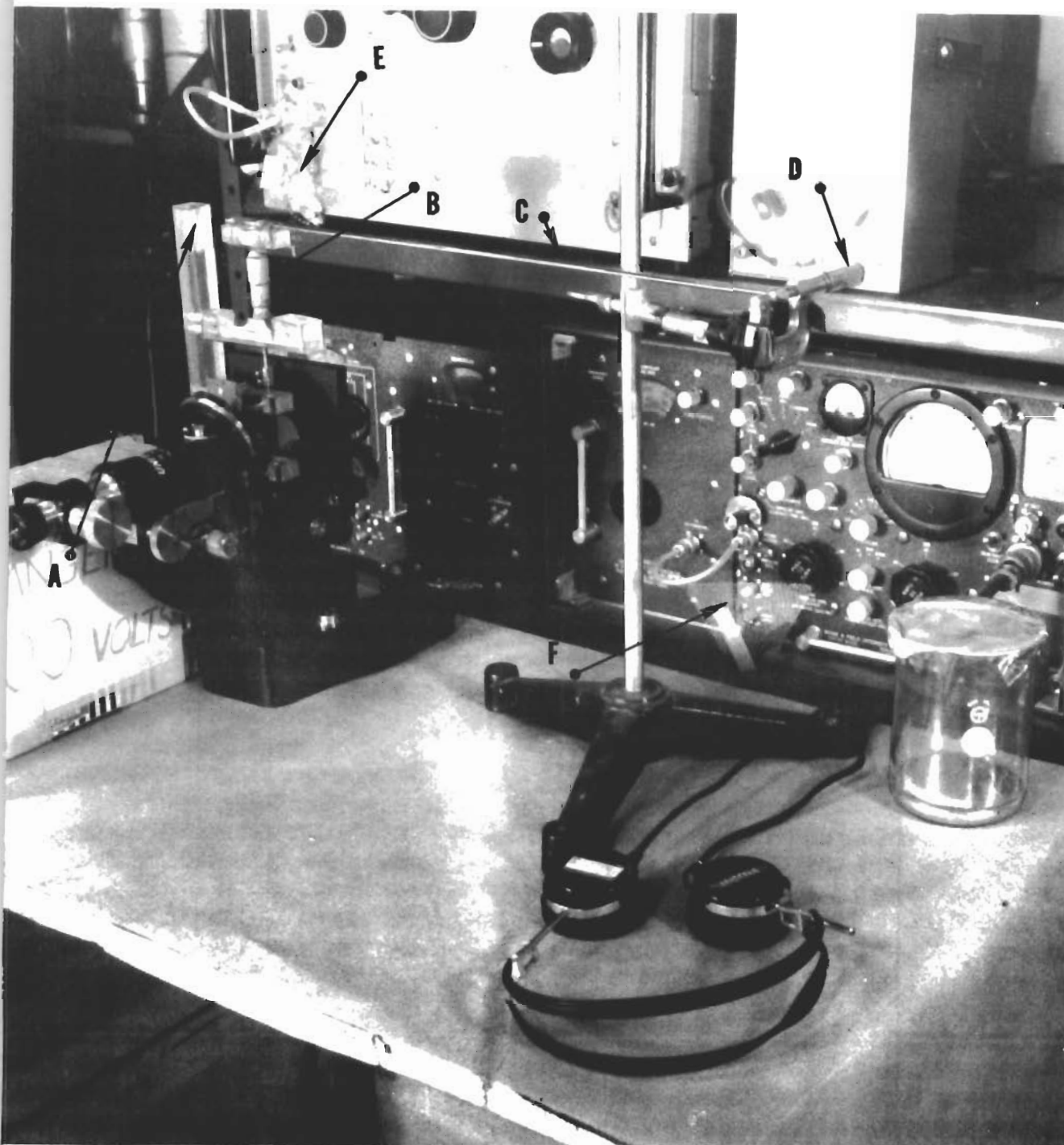
Figure 23. Micrometer Caliper-lever System for Adjusting Very Small Gaps. A - Electrode Support; B - Micrometer Caliper Adjusting the Gap; C - Lever; D - Micrometer Caliper for Adjusting Lever; E and F are Antennas Connected Directly to the Spectrum Analyzer and Noise Meter Respectively. Antennas 4 Inch Equalateral Triangles of Copper Screen.

A USEFUL VIBRATION SYSTEM

In this report it was postulated that malfunctioning compon-
ents which gave off rf radiation when tapped did so because a very
small gap existed in the component. It was noted that a "sharp tap" was
required, not the usual vibration. It was necessary to produce a high
acceleration equivalent to a "sharp tap" such as dropping the compon-
ent on the cement floor. As time was a very important factor in
producing a device which would furnish this requirement, the follow-
ing set-up was devised, Figure 24. A small bolt A was secured
on the shaft of a 1/4-horsepower induction motor B to produce
unbalance. The motor was No. 19361 made by Burke Electric Co.
with a no-load speed of 3600 rpm. The speed was controlled with
a variable 30 ampere transformer, not shown. By varying the speed
of the motor, mechanical resonance of the box and motor was ob-
tained. This was determined by the amplitude of the waves on the
mercury surface, D, by placing the hand on the box surface at F,
or listening to the vibration sound emanating from the box. The
motor was not fastened to the box. It did not appear to travel on
its base when in use. With this device, large sharp amplitudes were
obtained to extend discontinuities of components and connections
and to produce rf radiation under operating conditions. The com-
ponent and/or chassis was fastened firmly with screws or bolts on
the top of the box at position F. With 44.5 volts on the motor, sharp
resonance of the box was obtained. The position F acted as a
vibrating diaphragm yielding sharp high amplitude motion which
was found satisfactory to investigate discontinuities.

COLD SOLDER JOINTS

It is very difficult to make, or find, a cold soldered joint
at will. Therefore, tests for rf radiation with low voltage were
made using solder spheres .10 inch in diameter. These spheres
were made by applying solder to the bottom of a vertically held nickel
electrode .050 inch in diameter. The solder was that ordinarily
used in chassis fabrication. The spheres were nicely shaped with
very smooth surfaces. These "solder electrodes" were placed
in the electrode support, Figures 22 and 23, mounted on the micro-
scope stage where the gap was observed at magnifications of 25x
and 100x. With 67.5 and 135 volts across the gap, adjustments for
a continuous brush discharge were found very difficult to make. It
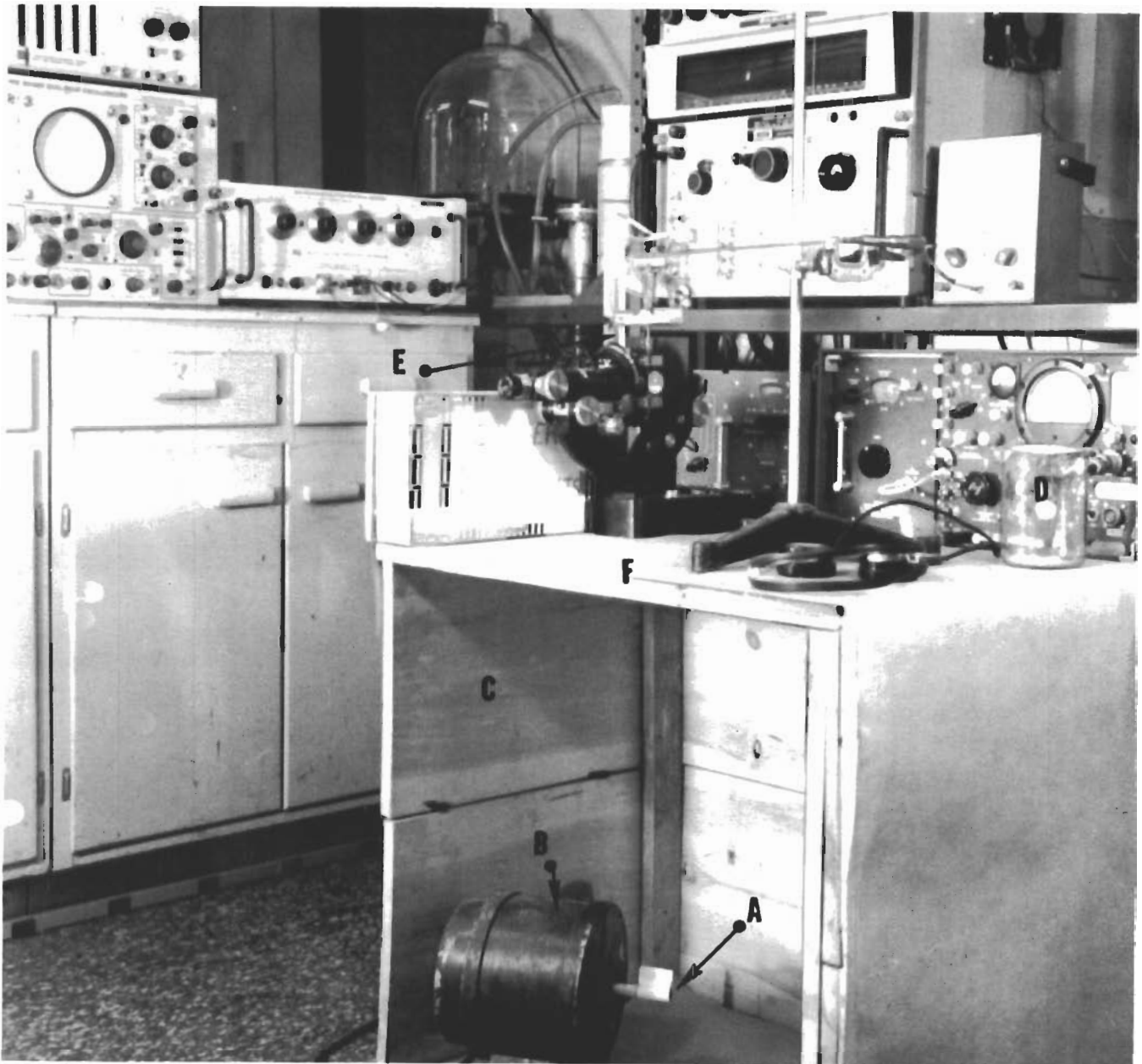had been noted previously with $\pm$ 500 volts across a gap, that the

Figure 24. A Useful Vibration System for Extending Gaps in Mal-
functioning Components and Connections. A - Bolt on Shaft to Produce
Imbalance; B - One-fourth Horsepower Motor; C - Wooden Box
27 Inch x 25 Inch x 14 Inch; D - Mercury Surface to Detect Resist-
ance; E - Gap Support on Microscope; F - Position for Mounting
Component Chassis.

61

gap could be adjusted to a maximum rf radiation output, that is
for a maximum number of discharges per second. The same number
of peaks in the frequency spectrum remained constant over this
adjustment range. For low voltages across very small gaps, it was
found necessary to provide a means of adjusting the gap to obtain
continuous discharge. A device for doing this has been described
above. The "solder" electrodes were viewed at a magnification
of 100x with back lighting of the microscope lamp set on "low".
As the gap was being closed with the device, the successive colors,
red, yellow and blue were seen. Closing the gap a very small addition-
al amount produced a continuous discharge. This occurred at a
gap spacing less than 4000A, the wave length of purple light. The
discharge could be obtained from gap settings over a range of 4000
Angstroms. The measuring device was not employed for making
absolute gap measurements. The gap separation must have been
of the order of a few thousand Angstroms (1 Angstrom = 10^{-8} cm),
i.e. less than 4000A. Gaps of this order of magnitude are found in
the study of electrical contacts[17]. The solder electrodes were
essentially in contact and therefore are representative of discon-
tinuities found in cold solder joints. That rf radiation was emitted
is shown by oscillogram in Figure 25. With the oscilloscope used
in this experiment the rise portion of the discharge is not shown;
only the decay portion is shown. The rf spectrum analyzer, noise
meter and rf radio verified emission of rf radiation from this very small
gap. This justifies the application of results on the larger gaps,
with dimensions of mils, to those of a few thousand Angstroms.

RESISTORS

The resistors tested for rf radiation were manufactured by
Ohmite Manufacturing Co.[18] and I.R.C.[19] They are designated
as carbon resistors. No chemical or instrumental analysis has been
made of them. As with the cold solder joints, a long search for
malfunctioning resistors with discontinuities was unsuccessful.
Therefore, it was necessary to induce discontinuities.

No discontinuities were found in resistors which were elect-
rically overloaded..

A 390 kΩ resistor was cracked with a hammer. Its resist-
ance became 2.7 megohms. Potential as high as 2000 volts dc battery
placed across it did not produce a discharge.
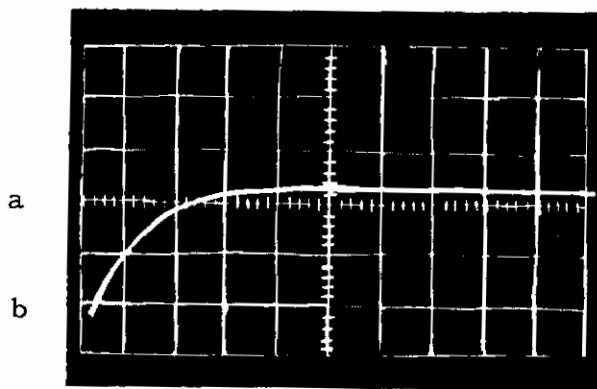
"Cold Solder Joint",
50 μsec/cm, .0005 V/cm

Figure 25. Oscillogram of RF Radiation from a "Cold Solder"
Joint. With the Oscilloscope Used, the Rise Portion, a b, of
the Trace was not Recorded.

A 470 kΩ, 2-watt resistor was broken in the middle, the potting trimmed away and placed in the electrode support, B in Figure 22. Potentials in 103.5-volt steps were placed across the rough surfaces. At 930 volts dc, a discharge was obtained and at 1030 volts dc, the discharge became a continuous arc discharge, i.e., not a brush type with avalanches. No rf radiation was detected by any of the measuring equipment using the highest sensitivities.

A 10 kΩ, 2-watt Ohmite[18] resistor was cut in half and ends were polished smooth. The ends were placed in the electrode support and connected directly to a battery. No effort was made to eliminate the outside covering of the carbon. With 828 volts a light blue discharge appeared, Figure 26. No rf radiation was obtained from the discharge. Later some rf radiation was obtained. The electrodes had become heated, some of the compound had melted and partially covered the carbon. It is believed the contamination on the carbon induced the rf radiation from the resistor.

To obviate the difficulty of contamination a 10 kΩ, 2-watt I.R.C. resistor was cut in half. The outside of the resistor was removed so that only flat-polished planes of carbon were exposed in the gap, Figure 27. The gap distance was essentially contact in the center to .00091 inch at the outer edge. The carbon electrodes were .072 inch diameter. The electrodes were viewed with a microscope with background lighting from the microscope lamp set on "low." A blue discharge was first observed with 415 volts across the electrodes. With 602 volts a large discharge was obtained but no rf radiation was observed. When 1035 volts was placed across cold electrodes, rf radiation was obtained for a few seconds. There was no rf radiation when electrodes became hot. Results are that no rf radiation was found from the electrical discharge between clean carbon I.R.C. resistors. Some rf radiation is emitted if the carbon is contaminated on its surface.

Carbon is an amorphous material giving a halo by the x-ray diffraction technique. Carbon exists in the crystalline form in graphite which gives a line diffraction pattern. It is of particular academic interest to determine whether crystalline carbon, graphite, emits rf radiation when forming the electrodes of an electrical discharge.

Electrodes were formed with two pieces of spectrographically

Figure 26. Discharge Between Plane Polished Surfaces of the Two Halves of a 10 K, 2 Watt Carbon Resistor, Gap Distance = .0025 Inch. Some RF Radiation Observed Due to Contamination.
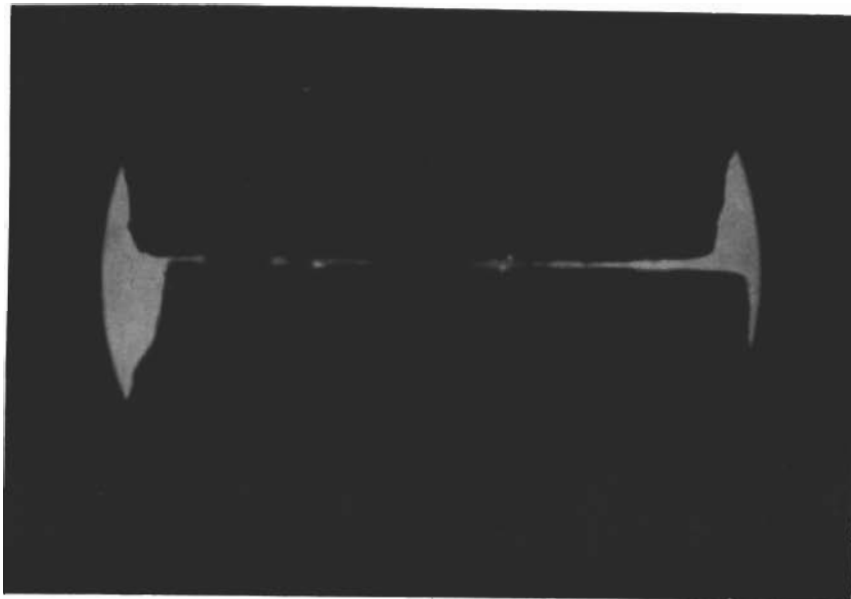

Figure 27. Discharge Between Carbon Electrodes Produced from the Halves of an IRC, 10 K, 2 Watt Resistor. Diameter of Carbon .0715 Inch, Gap Distance from Contact to .0009 Inch. No RF Radiation was Obtained. Bright Spots Possibly Incandescent Particles.

pure graphite[20] 1/4 inch in diameter by 1/2 inch long. These pieces were adapted to the electrode mount. The electrical circuit consisted of batteries with a 100 kΩ current limiting resistance and the electrodes. Radio frequency radiation was detected at 135 volts but the discharge was difficult to maintain. Rather than using the special device for adjusting small gaps, data were taken at 621 volts, gap distance .039 mm with 670 discharges per second. Radio frequency radiation peaks were observed on all receiving instruments. Representative rf radiation peaks from the graphite brush type discharge observed twice by one person with the noise meter are listed below. The amplitude data are estimated through use of the panel meter on the instrument. The background rf radiation make's it difficult to obtain accurate amplitude readings:

Observation I		Observation II		Frequency Difference	
Frequency Mcps	Amplitude Arbitrary Units	Frequency	Amplitude	(mcps)	(%)
22.5	13	23	7	+ .5	2.2
25.7	6	25.5	5	- .2	.78
42.0	13	42	7	0	0
65.5	12	64.5	8	-1	1.5
100	16	100	12	0	0
118	11	113	12	-5.0	4.2
		127	17		
135	11	135	12	0	0
147	11	143	14	-4	2.7
156	12	156	13	0	0
185	16	185	18	0	0

From these two sets of data, it can be seen that peak frequency determinations can be made to better than 4% of the reading, and that the graphite, a crystalline material, yields an rf spectrum and from previous data carbon resistors, an amorphous material, does not.

TRANSISTORS

Transistors which malfunctioned were collected over a period of one year from SRL's electronics laboratory. No discontinuities

were found and these transistors could not be used to demonstrate rf emission. It was, therefore, necessary to induce discontinuities in these components.

Figure 28 shows a germanium transistor 2N169 the crystal of which was broken. The discontinuity was scarcely visible to the unaided eye. The transistor was tested in the circuit shown in Figure 29. The transistor vector board was bolted near the transistor on position F, Figure 24, of the vibrator described above. With the vibrator in operation, an average of 500 electrical discharges per second were obtained when the discontinuity was opened. When the discontinuity closed during the revibration cycle, the transistor showed "normal" operation by the intermittent collection current indicated on the meter. When not vibrated this transistor showed open circuit and rf was not obtained.

The horizontal terminal connecting the crystal to the vertical electrode was broken in germanium transistor No. 2. Again the break was almost invisible. When vibrated as transistor No. 1 above, it then showed rf radiation by the rf receivers and "normal" operation by the intermittent current registered on the collector meter.

The third transistor tested was also a 2N169 germanium transistor. The crystal was broken on both sides of the whisker. This portion of the crystal fell out and was suspended by the whisker. The suspended portion of the crystal was replaced exactly into position. When vibrated an electrical discharge of 70 pulses per second was obtained and five rf radiation peaks were registered. It operated intermittently as indicated by the collector current.

Transistor No. 4 was known to malfunction. Upon testing it, no rf radiation was emitted even with sharp tapping with a screw driver. Thus, there were no discontinuities.

A new transistor was tested on the vibration table. Again with sharp tapping, no rf radiation was detected, even with the highest sensitivity setting of the detecting instruments. Therefore, there were no discontinuities.

POTENTIOMETER

The following potentiometer was tested. It is designated as Ohmite Type AB, 3500 ohm, 2-watt, Allied Electronic catalog

TRANSISTOR
BREAK

NPN CRYSTAL

COLLECTOR
POST

EMITTER POST

WHISKER

BASE POST

C

E

B   B

2N169 TRANSISTOR
TOP VIEW

TRANSISTOR
BREAK

NPN CRYSTAL

COLLECTOR
POST

WHISKER

TOP ENCLOSURE
(CUT OFF)

BASE POST

EMITTER POST

BOTTOM
ENCLOSURE

C   E

B   B

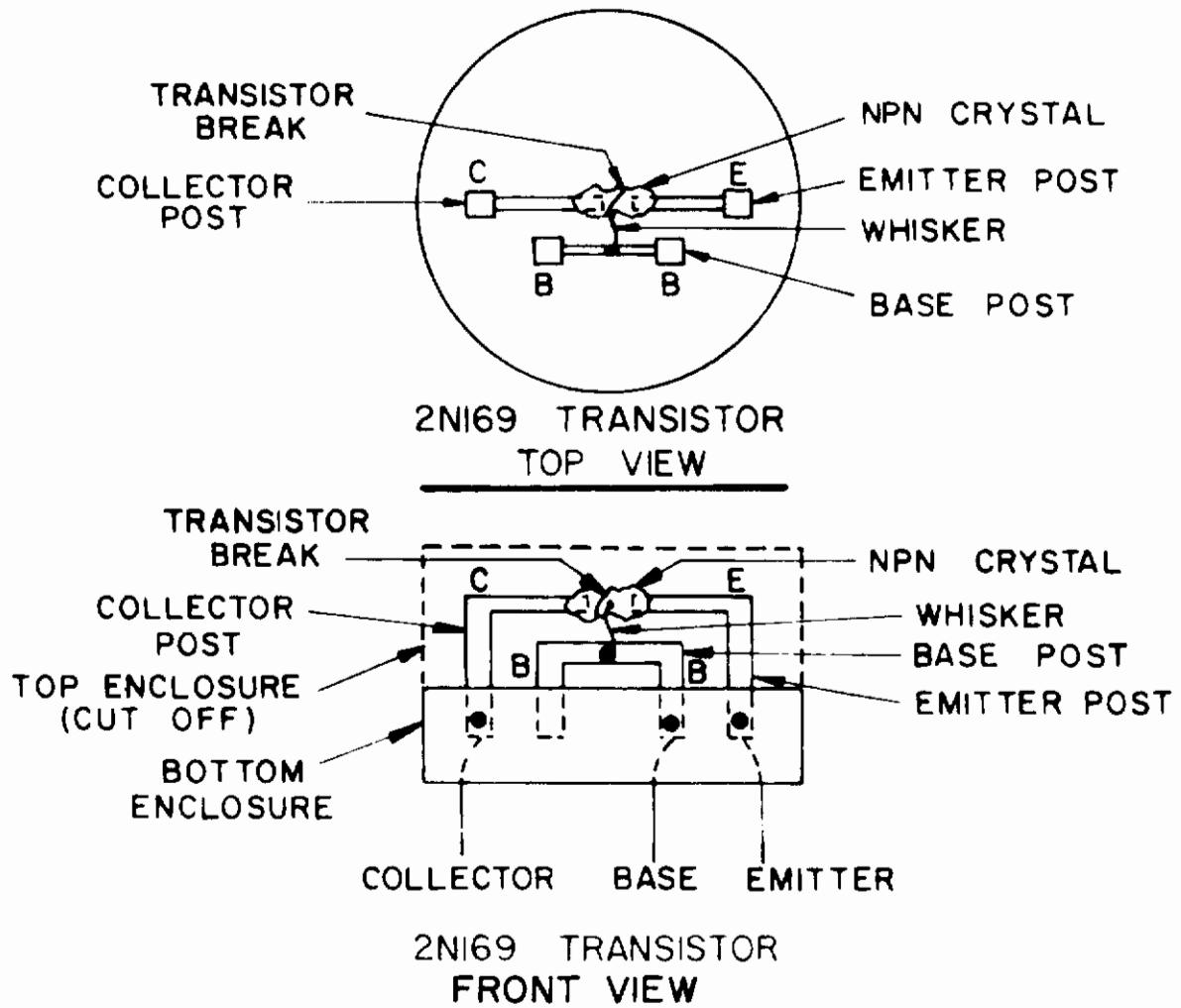COLLECTOR   BASE   EMITTER

2N169 TRANSISTOR
FRONT VIEW

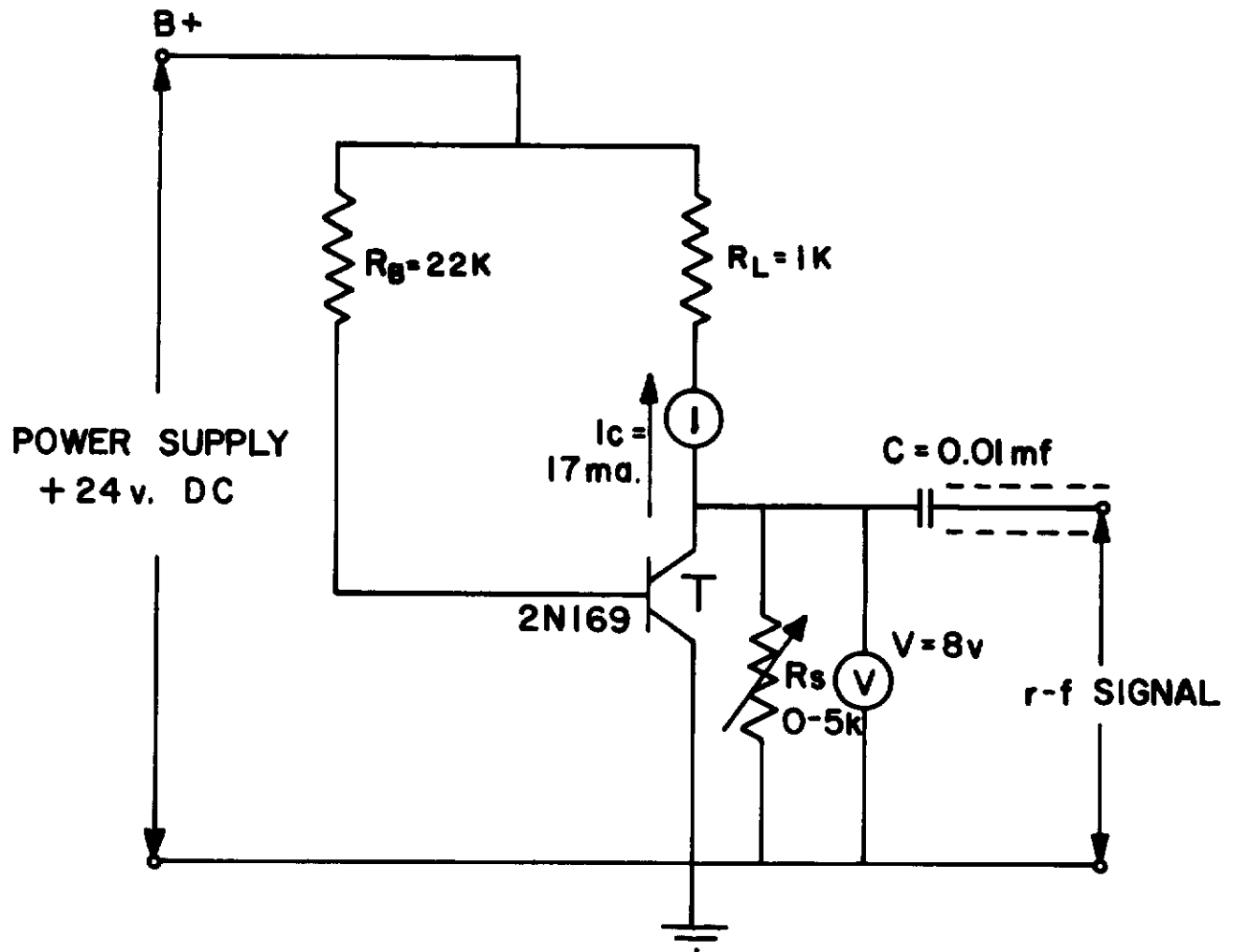Figure 28.   A Transistor Broken for Discontinuity
Tests

Figure 29. A Circuit Employed for Testing Transistors With
Discontinuities.

69

No. 28M600, Manufacturer's Type CU3521. Type AB is a molded composition resistor with a carbon contact. This potentiometer was made to malfunction by placing an electric overload on it. The area between the carbon brush and the composition resistance burned and destroyed the resistance. The contact was moved near the undamaged composition resistance. Radio frequency radiation was obtained with a battery potential of 585-1000 volts across the contact. The peak radiation of the potentiometer carbon-composition gap is compared with the graphite-graphite gap in Table 6. The data were taken by the same person on the noise spectrometer with the same antenna inserted in the input socket. The generation circuit for both potentiometer and graphite consisted of a battery, a current limiting resistor, and the rf generator. The voltage for the potentiometer circuit was from 585 to 1000 volts, the graphite 621 volts. Since the experimental conditions are essentially the same, this data should be comparable. It appears that certain peaks may be representative of the electrode material while others found in both columns represent the generator and/or receiving circuit oscillations.

DIODE NO. 1

Diode No. 1, not marked, was similar to silicon diode 1N923. There was a very small break of .2 millimeter in the gold wire whisker. A 7x magnifying glass made the break visible. The generation circuit consisted of a 1000-volt battery, 100 megohm resistor and the diode. An electrical discharge was obtained with 300 pulses per second and a current of 10 microamperes. Radio frequency radiation was obtained and in greater amplitude when the crystal was connected to the positive battery terminal. The peak frequencies for the diode gold whisker and for gold electrodes .050 inch in diameter are shown in Table 7. The agreement between frequency measurements is good. No explanation is given for the two missing frequencies.

Diode No. 2 was similar to a 14191. The glass envelope was scribed circumferentially with glass cutter. It was broken in two pieces and the gold whisker detached from the crystal. The diode was reassembled with the gold whisker resting upon the crystal. The glass parts were adhered with Duco cement. The diode was placed in series with a 5 megohm resistor and 63 volts battery. When placed on the vibrating table, or tapped, the oscilloscope indicated a scratching type action of the gold wire across the crystal. No rf radiation was obtained with the voltage used.

70

Table 6

Comparison of Peak Frequencies of Radio Frequency Radiation from a Malfunctioning Composition-Carbon Potentiometer and a Graphite-Graphite Electrical Discharge			
Potentiometer		**Graphite**	
Frequency Mc/sec	Estimated Amplitude	Frequency Mc/sec	Estimated Amplitude
21 -	S	22.5 -	13
		25.7 -	6
35 -	S		
42.5 -	S	42 -	13
52 -	W		
67 -	A	65	18
		100	12
		113 -	12
125 -	W	127 -	17
		135 -	12
		143 -	14
		156 -	13
164 -	VW		
184 -	VW	185 -	18
203 -	VW		
S = Strong, A = Average, W = Weak, VW = Very Weak			

Table 7

Peak Frequencies Obtained with the Noise Meter for a Discontinuity in the Gold Whisker of a Diode and Pure Gold Electrodes			
Diode Similar to 1N923		Gold Electrodes	
Frequency Mc/sec	Estimated Amplitude	Frequency Mc/sec	Estimated Amplitude
22	20	22.5	14
27.3	15	27.3	14
35.6	8	35.2	10
42.4	10	43.0	9
49.0	12	——	
——		56.2	16
62.0	8	65.0	3
71	8	71.0	10
79	16	79.0	5
87	3	89.0	9

MISCELLANEOUS COMPONENT STUDIES

A number of electrical components and devices were taken at random and subjected to tests for rf radiation. They are discussed below. A resume of the results of the experiments are given before the detailed discussion.

Resume of Results of Component Studies

Type of Component	Rf Radiation emitted in range of 10-1000 mcps
Capacitor	No
Vacuum Cleaner Motor	Yes
Diode (fixed spacing break)	No
Potentiometer	Yes
"Washing Machine" Motor	Yes
Resistor (Carbofilm)	Yes
Resistor (Ohmite Carbon)	No
Interrupter (Chopper)	Yes
Vacuum Tube	No

DETAILED DISCUSSION OF COMPONENT STUDIES

Capacitor

Attempts were made to initiate breakdown in two capacitors under operating voltage and under excessive voltage applications in order to produce the emission of rf radiation. Relatively high leakage currents could be produced and the current (monitored by a cathode ray oscilloscope) through the capacitors could be varied by tapping them. The current variation was, however, a continuous type which varied abruptly in amplitude upon tapping. Attempts to induce discrete breakdown channels to produce an intermittent breakdown failed even when operating the capacitors 600% above their nominal (dc) working voltage. In this instance, they were cooled with dry ice to prevent massive ohmic heating damage.

73

Vacuum Cleaner Motor (Brush type - ac)

Radio frequency emission (profuse) was noted in the 20 to 430 Mc/sec range of the spectrum. Peak frequencies were detected with the noise meter and the spectrum analyzer.

Diode (rectifier - 1N87G)

The glass case of a diode was broken apart , the whisker pulled from the crystal, and then placed back against it. The case was then sealed together and the usual voltage applied. Current monitoring indicated continuous although abrupt variations in the current when vibrating the entire unit. No rf radiation was observed. This experiment may be compared with the similar experiment above.

Potentiometer

A 50 kΩ potentiometer (variable resistor of the deposited film type using a "carbon" like electrode on the moving arm) was connected in series with a 12-kΩ carbon resistor to a 20-volt dc battery. Vibrating the potentiometer caused rf emission to occur. The vibration had to be of very large amplitude. The surface between the moving brush and resistive surface was then destroyed by an excessive current. This approximated a noisy, defective potentiometer. When the brush was over the "burned" area, rf radiation peaks, and background were obtained. These were induced by light vibrations of the potentiometer.

Induction Type 1/4 HP Motor

The motor B, Figure 20, was run at variable speed with a variable transformer. Radio frequency radiation peaks and background were observed at all speeds. The motor, which is essentially enclosed, was placed on a 2-foot x 5-foot copper screen. An antenna, E and F in Figure 23, was inserted into the female end of a 27-inch co-axial 50 ohm cable which was connected to the attenuator input of the SPA spectrum analyzer. Peaks were found at 26 and 171 Mc/sec.

Resistor

An Aerovox carbofilm resistor, 2-watt, 100 kΩ , type EPX was broken in half and smoothed with No. 0 metallographic paper. The resistive film covers the outside of the cylindrical insulator which in

74

turn is covered by a glazed insulation material for protection. The two halves located 0.01 inch apart formed the gap. A potential of 2000 volts was applied in series with a 100 megohm resistor and the "broken" resistor halves. Radio frequency was detected on the cathode ray oscilloscope using a triangular screen antenna. When the two halves were rubbed together, rf radiation was obtained using only 135 volts. This occurred because of the smallness of the discontinuities from the rubbing action. These results tend to indicate the resistive film was crystalline rather than an amorphous. The nature of the film has not been determined.

Resistor (Ohmite granular carbon - 15 megohm, 1 watt)

The same type of experiment was performed as above. No rf was observed. This is in accord with previous results obtained in the attempt to obtain rf emission between carbon electrodes in air at high potential. Scratching together, make-break, other tactics were tried but no rf was obtaind.

Chopper

A Hughes Airpax A 589-3 6-volt, 400 cps chopper was operated with 100 volts on the vibration contacts. The chopper was located 12 inches from the spectrum analyzer and the noise meter used with triangular antennas on their input. Both a 100-volt battery and stablized power supply were used. Identical spectral peaks were obtained for each power supply for a given receiver.

Vacuum Tubes

Attempts to produce rf emission from vacuum tubes (pentodes and triodes) under conditions and in circuits in which they normally operate, as well as in operation far above recommended potential levels, were futile. Tubes which exhibited gaseousness emission (blue gas glow) were examined for rf emission, but none was observed, even under the most ideal sensing arrangements of the receivers. The reason for these results is that rf radiation emission depends upon obtaining a brush type discharge which depends upon the field and the gas pressure, $\frac{E}{p} \left(\frac{volts}{cm\ torr}\right)$. These conditions did not prevail in the tubes tested. Discontinuities also may not have been present. Radio frequency has been detected from loose tube prongs and their socket. Under these conditions, the $\frac{E}{p}$ value can be obtained for a brush type discharge.

## Radio Frequency Detection of Radio Receiver Fault

Radio frequency peaks generated by an electrical discharge from nickel electrodes in air were being studied with three receivers. These receivers were the Hallicrafter radio receiver SX62A; the Singer Spectrum Analyzer, Model SPA-4a, and the Empire noise meter Model NF105. Each receiver was connected to a small antenna, Figure 9. The antennas were positioned in a cluster four feet from the electrical discharge. Each antenna consisted of a copper screen equilateral triangle, two inches on each side, soldered with its plane perpendicular to a copper wire. The wire was inserted into the female end of a shielded cable which led to the receiver..

During the course of the study, the sensitivity of the Hallicrafter receiver had been advanced above position 8 on the 10 position dial. A very unusual pattern happened to appear on the spectrum analyzer. The radio receiver had been previously set at 15.5 Mc/sec when this occurred. The spectrum analyzer picked up with its antenna the signal radiated from the receiver antenna. Figure 30 shows four frequencies received: 12.7, 86.0, 165 and 330 Mc/sec. It will be noted that the relation of the frequencies are 7, 13 and 26 times the first frequency. The frequency band with side lobes are recorded in the pictures (1), (2) and (4).

Of much interest is the fact that pictures (1) through (4) showed almost continuous spikes or energy bands. By diminishing the signal with the sensitivity dial, energy bands could be shown more clearly, picture (5). The question arose: are the energy bands actually coming from the oscillating circuit of the receiver or are they a function of the sweep frequency of the spectrum analyzer? Since the spectrum analyzer had been giving some operational problems, it was decided to pursue this question further.

A 10-Mc/sec signal from a signal generator was connected directly with a cable to the spectrum analyzer. The record of the spectrum analyzer is shown in picture (7). Picture (8) indicates the output of the signal generator was a sine wave. This evidence demonstrates the signal generator was operating satisfactorily and records a sine wave as such. The energy bands given out by the oscillating receiver, picture (5), are therefore, real and are not a function of the sweep of the spectrum analyzer.
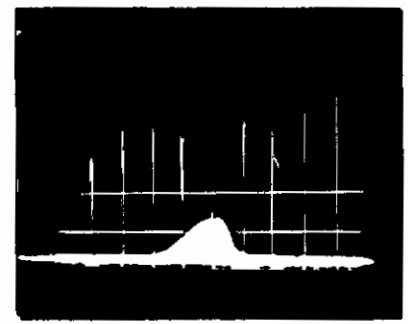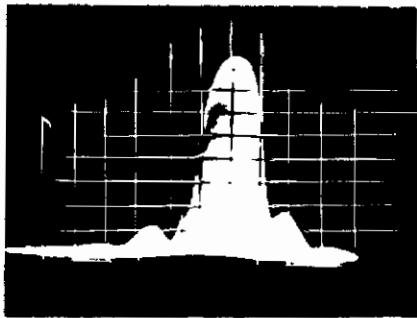
76
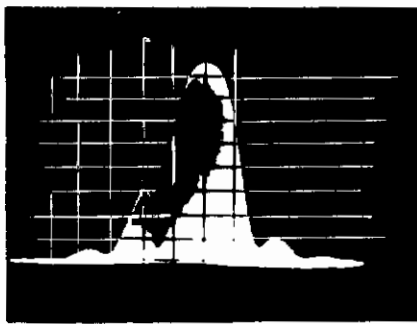
(1)
12.7 mcps
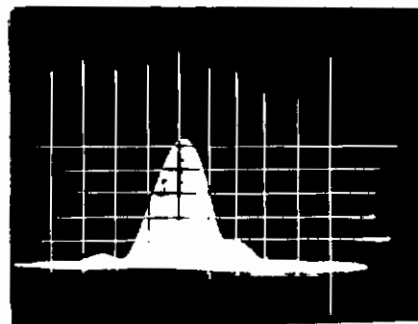
(2)
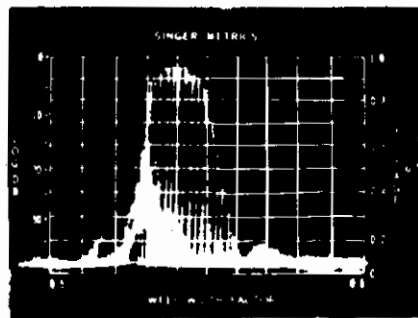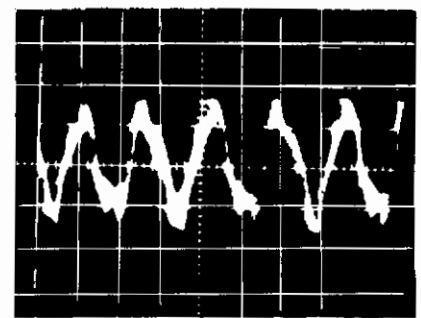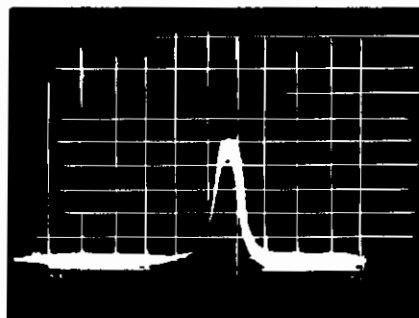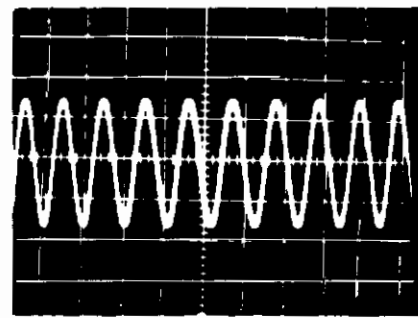86.0 mcps

(3)
165 mcps

(4)
330 mcps

(5)
12.7 mcps

(6)
.1 μ sec per centimeter

(7)
10 mcps
Spectrum Analyzer

(8)
10 mcps
Oscilloscope

Figure 30.   A Study of RF Radiation from the Short-wave Receiver
Forced into Oscillation Between 15 and 18 Mc/sec by Advancing the
Sensitivity Dial from 8.9 to 10.   Pictures 1 Through 4 Show the
Frequencies with their Side Lobes Taken on a Spectrum Analyzer.
Picture 5 Indicates the Discrete Frequencies of Which Each the Four
Peaks Above are Constituted, but Not Readily Visible.   Picture 7
Shows the Record of the Spectrum Analyzer of a 10 Mc/sec Sine-
wave; Picture 8 Shows an Oscilloscope Trace From the Signal Gener-
ator; Picture 6 Shows a 11 Mc/sec Signal From the Receiver on an
Oscilloscope, Scale .1 Microsecond Per Centimeter.   This Corres-
ponds to the 12.7 Mc/sec Shown in Picture 1.   Scales for Pictures
1 Through 5, 2 Mc/sec = 10 Divisions.

One possible explanation of this phenomenom is the local oscillator of the receiver was set into forced oscillation. Radiation from the receiver antenna was picked up by the antenna of the spectrum analyzer. Picture (5), Figure 30, shows a number of spikes or energy bands which form envelopes in four positions on the frequency scale of the spectrum analyzer. Each band is interpreted as being due to a group of electrons having the same velocity or energy. Thus each envelope forms an energy distribution of electrons over a particular frequency range. The envelopes for the receiver occur at frequencies having harmonic relationship. The source of electrons from which the peak frequencies are derived must come from the current in the oscillating circuit.

To summarize the studies of rf detection of radio receiver faults:

(1) A receiver was found to "malfunction" through rf radiation emitted from its antenna.
(2) Four frequencies were found from 12.7 to 330 Mc/sec.
(3) These frequencies consisted of peaks and side lobes.
(4) Spikes or energy bands were found in each peak.
(5) The energy bands were shown to be real and are assumed to come from the oscillating current of the receiver.

78

Section 5

DISCHARGE MECHANISMS

The objective of this study was to learn more about the gaseous discharge mechanism in order to implement rf radiation check-out of electronic components and connections.

It has been shown that the rf radiation comes from discontinuities in components and connections of several thousand angstroms spacing, ca 4000 Angstroms. It has further been demonstrated that phenomena occurring in the very small gaps could be represented by phenomena in larger gaps, .5 to 10 mils. The latter gap sizes were employed for the mechanism studies.

In studying the electrical discharges, currents were measured from 10^{-12} amperes to 1 milliampere. It was found that the type of discharge most applicable to that occurring in malfunctioning components was the brush type discharge. This discharge includes the formation of a high conductivity path between the electrodes by avalanches and streamers but does not necessarily include the vigorous spark which also was shown to produce rf radiation. If a spark occurred between components, it would be quite obvious where the malfunction existed. However, the brush discharge is quiet to the ear for very small gaps and low currents. It is usually invisible; yet it emits rf radiation. This is the type of discharge one would expect to exist in malfunctioning electrical devices. Figure 31 shows a very low current discharge which emits rf radiation. The discharge is essentially invisible to the unaided eye.

There are two fundamental processes by which the distance between electrodes can be made electrically conductive.

The first process is the Townsend mechanism. It is a slow mechanism depending upon a cascade multiplication of positive ions. The more rapid mechanism develops an avalanche from a single electron which itself may produce breakdown. It has been established that the avalanche type of breakdown is the important mechanism for producing rf radiation from discontinuities. First, the rise time for the discharge is in the nanosecond range, and second, assuming a single electrical pulse is a single avalanche, data for Townsend's
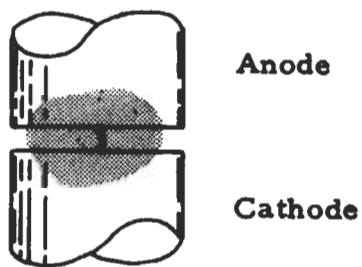
79

Anode

Cathode

Figure 31. Photomicrograph of a Low Current Discharge Between Nickel Electrodes. The Series Circuit Contained 1700 VDC Battery, 5000 Megohms and the Electrodes. There were 12 Discharges Per Second. The Discharge is .68 Mils Wide, the Bright Sphere on the Cathode is .91 Mils Diameter and the Gap Separation is 8 Mils, at 730 Torr. The Cathode is the Electrode in Subsequent Photomicrographs.

first coefficient "α", has yielded reasonable results. Other experimental data also contributes to this conclusion.

Experimental evidence indicates that a single electron is produced by the field emission mechanism. This electron is amplified by the avalanche process according to $n_o = n_o e^{\alpha x}$. In this case $n_o = 1$. By increasing the field, the discharge rate increases. In this case, $n_o \gg 1$ and there are a number of avalanches which grow and produce the breakdown. The avalanche may begin with a ball of white light on the cathode, travel across space in the gap to anode, and end there in a small ball as in Figure 31. In some cases, it may terminate on the anode without the ball, but with numerous minute "pin point" discharges just visible under the microscope at 100x. This was the case when 1500 volts dc, 100 MΩ, and nickel electrodes separated 10 mils were employed in series. Viewing the plane faces of the electrodes at 100x magnification, it was noted the cathode had very fine pits over its surface with a depression where the discharge was maintained. The anode surface was also covered with a fine etching effect and a small raised portion. The raised portion is approximately located in a position opposite the depression in the cathode and may be caused by ion sputtering of the cathode onto the anode. There was a small diameter hole on both electrodes due to a single discharge path. The hole was deeper on the anode. This experiment indicated that electrons are very active in the discharge but $+$ ions must also be considered.

Another different discharge which emits rf radiation is shown in Figure 32. Balls of visible white light are seen on the cathode which is also covered with cathode glow. Crookes dark space is seen followed by a positive column. The discharge was in air at atmospheric pressure at a higher current density than the one above, i.e., 1900 volt dc battery in series with a 1.5 MΩ resistor, and nickel electrodes. Other data may be found in Figure 32. The dark space is a free path for electrons to gain velocity to produce ionization. It is .91 mils or 2.3×10^{-3} cm. A free path calculated from $\frac{1}{\alpha}$ obtained from measurements of transient phenomena yield 1.25×10^{-3} cm which is on the order of magnitude. A discharge emitting rf is obtained without balls of visible white light as shown in Figure 33. Data for this discharge is shown in the figure. It will be noted the
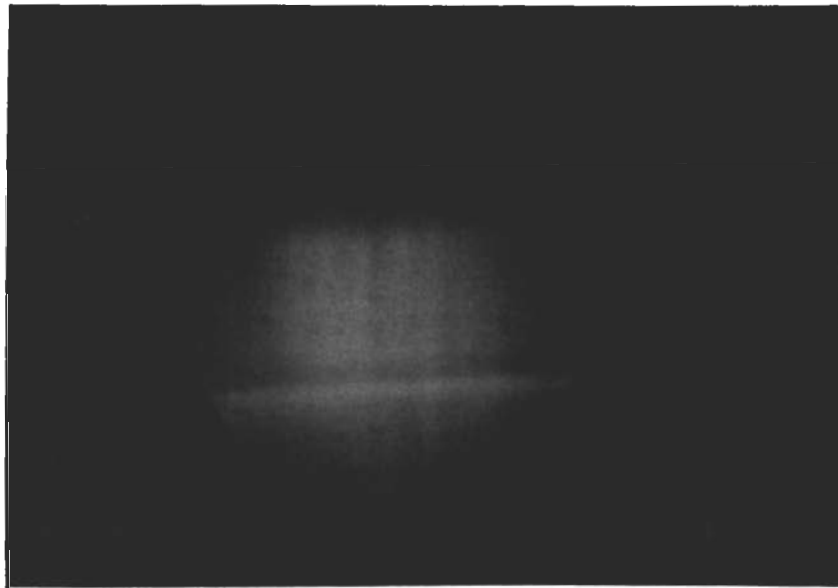
Figure 32. Photomicrograph of a Discharge Between Nickel Electrodes
in Air at 730 Torr and Higher Current than Figure 31. Series Circuit
Contained 1700 VDC Battery, 1.5 Megohms and .050 Inch Diameter
Nickel Electrodes. Other Data: Gap 7.7 Mils, Cathode Glow .14
Mil, Balls on Cathode .91 Inch Diameter, Dark Space .91 Mils
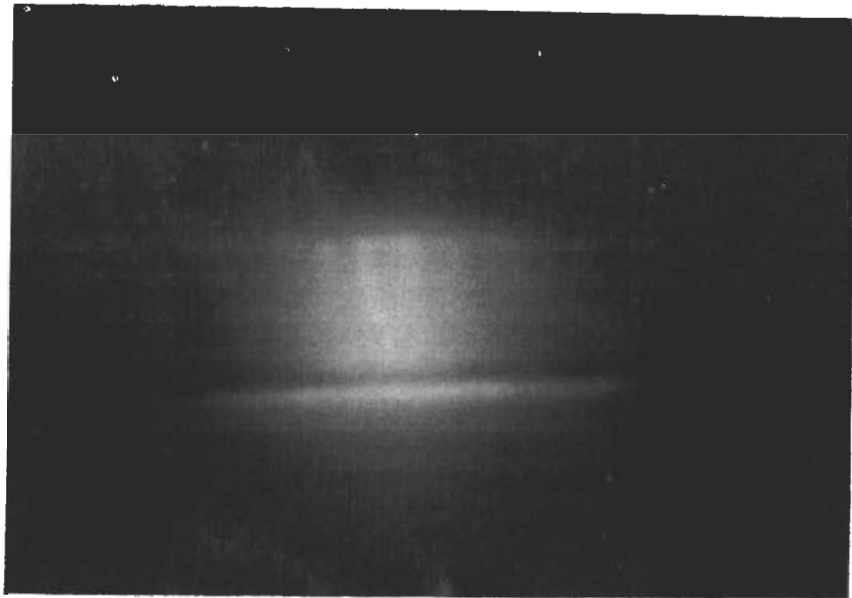$(2.3 \times 10^{-3}$ cm).

82

Figure 33. Photomicrograph of an RF Generating Discharge at Atmospheric Pressure Without Balls of Visible Light on the Cathode. Note: "Cones" of Discharge Originating at the Anode. Series Circuit 1700 VDC Battery, 4.5 Megohms, Nickel Electrodes, Gap 7.7 Mils, Cathode Glow .15 Mil, Crooks Dark Space .45 Mils (1.14×10^{-3} cms).

current in this discharge is slightly less than that in Figure 32 because of the larger current limiting resistor. The dark space is smaller. The pressure for both discharges was nominally 730 torr. A different phenomenom appears in this figure; a cathode seeking discharge initiating at the anode is visible. (The front dimensions are top .91 mils, bottom 1.82 mils, length 6.60 mils). This "cone" of discharge could be a positive ion space charge traveling toward the anode. It could also be an avalanche type discharge originating near the Crookes dark space and traveling toward the anode. Figure 34 shows nickel electrodes with balls of white light and cathode glow, the dark space and a positive column. The "cones" of discharge are also shown. This photograph thus exhibits a cathode glow, balls of white light, a dark space, white cones surrounded by blue light. Data are shown in the figure. It appears that the white light from the white cones from the anode has diffused into the blue "positive" column.

Figures 31 to 35 show types of discharges obtained which emit rf radiation. The gap distance is so small that in the present investigation, the type carriers in the different parts of the discharge could not be readily determined. In future work, the gap will be extended in an attempt to obtain these data.

The above discussion about the part played by field emission and the avalanche as the important mechanism of the rf emitting discharge did not take into account secondary electrons and their origin. With the visible and ultraviolet light present in the discharge, secondary liberation of electrons from the cathode is important. Photoelectric ionization in a gas can be made by photons produced in the primary avalanche. Also very important is the liberation of electrons by impact of positive ions on the cathode, γ_i. While electrons appear to be the most effective agent in producing the breakdown, positive ions must be considered. Positive ions will effectively shorten the gap extending from the anode to within a short distance of the cathode. Thus, field emission from the cathode will be increased. Positive ions produced in the avalanche will also increase the field effect.

Further justification of the avalanche mechanism of breakdown is the fact that numerous calculations of parameters based upon this mechanism have given satisfactory answers in most cases. Details of this mechanism and other contributing factors will be studied

84

Figure 34. Photomicrograph of a Discharge Between Copper Electrodes
.050 Inch Diameter Showing Cathode Glow, Balls of White Light,
Dark Space Cones of White Light Diffused into the Blue Discharge
in the Vicinity of the Anode. The Series Circuit Consisted of 1300
VDC Power Supply, 15 Megohms and the Electrodes. Other Data:
Gap 10.2 Mils, Cathode Glow 1.36 Mils, Dark Space .91 Mils,
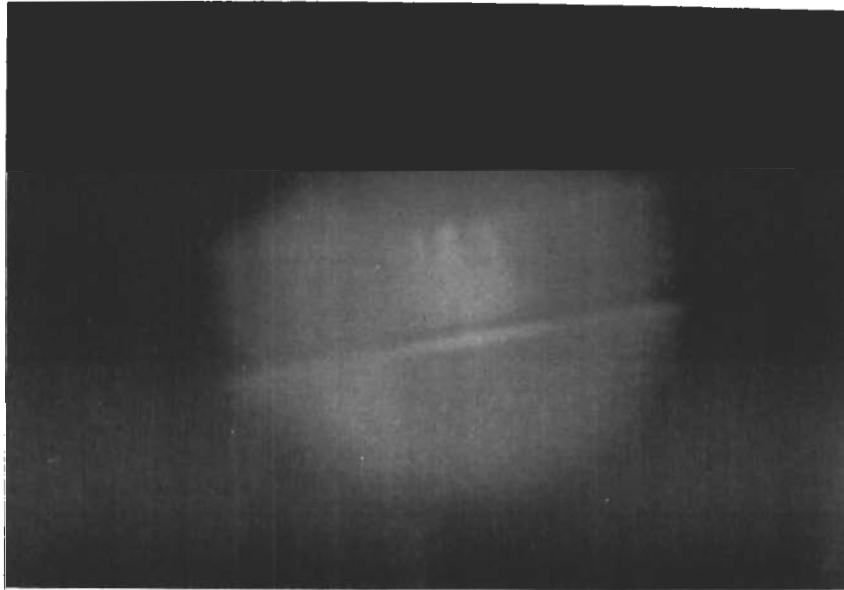Column 7.9 Mils.

85

Figure 35.   Photomicrograph of One Type of Electrical Discharge Between .050 Inch Diameter Nickel Electrodes in Air at 730 Torr Pressure.   The Gap is .0077 Inch, the Negative Glow .0006 Inch, Crookes Dark Space .00045 Inch, Cone from Anode .00091 Inch Top, Bottom Approximately .0025 Inch, and Altitude .0066 Inch. The Series Circuit Consisted of 1700 Volts Battery, 1.5 Megohms Current Limiting Resistor and the Nickel Gap.

further employing different electrode materials, gases and pressures
in uncomplicated discharges like that shown in Figure 31. Though
the rf radiation spectral peaks are considered to be influenced by
the electronic generation and receiving circuits, experiments have
shown that the peaks may be shifted, added to, or taken from the
spectrum by changes made in the electral discharge. Measurements
made with the spectrum analyzer (volts vs. frequency) show spikes
or energy bands in the background and in the peaks. Each energy
band is interpreted as representing a group of electrons having the
same velocity of energy. A peak is thus an energy distribution
of electrons. The electrons giving off the rf radiation can be found
in both the oscillating circuitry and within the gas discharge.

Section 6

SUMMARY

EXPERIMENTS

The emission of rf radiation has been studied over a range of frequencies from .15 to 400 Mc/sec for small gaps of .5 to 10 mils between electrodes .050 inch in diameter, with polished flat surfaces. Most of the later work was done with nickel electrodes in air at atmosphereic pressure though other materials such as gold, copper, and aluminum were used for electrodes and argon was used as a gas.

During these experiments, considerable effort was expended upon shielding apparatus from unwanted rf noise, determining effects of cables, antennas, generator and receiver circuitry upon the rf radiation spectral peak measurements with the instruments and study of the discharge characteristics which produced rf radiation. As time progressed, numerous experimental problems were solved and reliable repetitive results could be made. Numerous experiments previously performed were then repeated with the improved technique.

A number of electronic components were caused to malfunction by introducing discontinuities. At low voltages, 28, 67-1/2, and 135 volts dc battery and up, the component gaps were very small. Gaps of the order of less than 4000 Angstroms were instrumentally determined. This gap separation is essentially contact. In fact, the ends of the two halves of resistors used as electrodes were rubbed together. The discharge obtained emitted rf radiation.

RESULTS

It has been demonstrated that rf radiation emanating from malfunctioning electronic components and connections comes from discontinuities in the components which are very small. The discharges, sometimes invisible to the unaided eye, were found to be the brush type which gives an rf radiation spectral background with peaks located at various positions in the spectrum. With the aid

88

of the spectrum analyzer, each peak was found to be made up of a
large number of spikes, or energy bands, which increased in amp-
litude and number as the field increased. Each energy band was
interpreted as coming from a group of electrons of the same energy.
Thus, each peak represents an electron energy distribution envelope
for its spectral position. The number of peaks made visible depends
upon the field applied across the discontinuity. For low fields, possibly
one or two peaks are detectable, for higher fields essentially all
of the peaks to be obtained become visible and increase in amplitude
with the field. The peaks obtained are a function of the electrode
material, the kind and pressure of the gas in the discharge, Figure 36,
the circuitry of the receiver and generator. The peaks related to
circuitry bear a rather accurate harmonic relationship which has
not been found for peaks originating from the discharge generator.
Experimental results indicate the avalanche type mechanism explains
the electrical breakdown in the discontinuity. This brush type discharge
can be so small as to be invisible to the unaided eye, yet it was found
to emit rf radiation. It can be found in malfunctioning components
and connections. The rf radiation comes from oscillating or accelerated
electrons. Experimental evidence indicates the source of these
electrons are within the electrical discharge and within the external
oscillating circuit.

A number of electronic components and connections were
demonstrated as emitting rf radiation from discontinuities. These
devices included: a cold soldered joint, transistors, diodes, potentio-
meters and film type resistors. No rf radiation could be obtained
from carbon resistors but it could be obtained from graphite.
(Carbon is amorphous, graphite is crystalline carbon). No rf was
obtained from the vacuum tubes tested.

Figure 36. Peaks in the RF Spectrum as a Function of Gas and Pressure. Generating Circuit Consisted of Battery, Current Limiting Resistor, and Ni Electrode. Electrode Separation 0.019".

AIR, P=716 mmHg, E=1700 volts

ARGON, P=710 mmHg, E=1300 volts

ARGON, P=452 mmHg, E=1300 volts

ARGON, P=452 mmHg, E=770 volts

ARGON, P=289 mmHg, E=770 volts
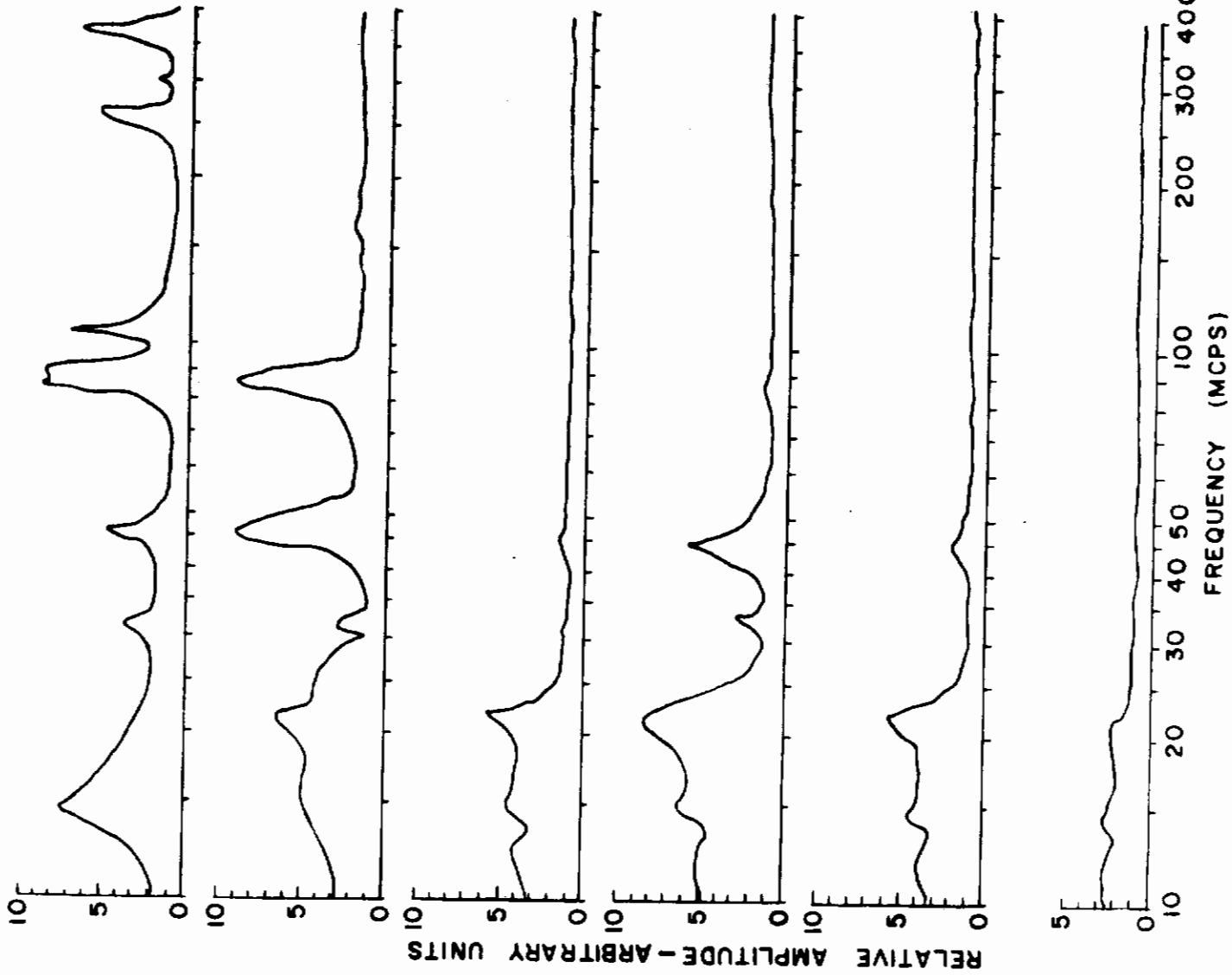
ARGON, P=220 mmHg, E=770 volts

RELATIVE AMPLITUDE—ARBITRARY UNITS

FREQUENCY (MCPS)

90

Section 7

CONCLUSIONS

A good understanding has been established for the generation of rf radiation from malfunctioning components and connections. Even though the discontinuities and discharge may be so small as to be invisible, rf radiation is emitted. Considerable information has been obtained about the peaks found in the rf spectrum.

For future work, it is concluded that the affect of various parameters on the rf radiation peaks must be investigated. Such parameters include the affect of electrode materials, gap separation, current levels, gap potential, atmospheric temperature, different gases, gas pressure, humidity, ionization by x-rays and ultraviolet light and use of magnetic fields. Information from these experiments will provide additional theoretical information as well as techniques to detect more efficiently than heretofore malfunctions in electronic systems. They will also provide a means of relating rf radiation peaks to specific components and devices.

APPENDIX A

APPENDIX A

EQUIPMENT USED IN LABORATORY EXPERIMENTS

1. The noise analyzer, The Singer Co., Empire Model NF105

2. The spectrum analyzer, The Singer Co., Model RF-4a

3. The receiver, Hallicrafter, Model SX62A

4. The oscilloscope, Tektronix 581-A

5. Receiver - Hallicrafters - Model S20R

6. Receiver - Hallicrafters - Model SX 62A

7. Speaker - Hallicrafters - Model R48A - Serial No. Q224F13

8. VTVM - Hewlett-Packard - Model 400A - Serial No. F2454

9. VTVM - Heathkit - Model AV-3

10. VHF - Signal Generator - Hewlett-Packard - Model 608D
    - SN 202-07732

11. Autotransformer - Powerstat - Model 20

12. Hi-Voltage Transformer - Jefferson Electric Co. - Model 721-111,
    SN 21864-2

13. VOMA Meter - Simpson - Model 260

14. Electrometer - Keithly - Model 621 - Serial No. 29005

15. DC Power Supply - Heathkit - Model PS-3

16. DC Power Supply - Heathkit - Model PS-4

17. Vacuum System - Kinney - Model SC-3 - Serial No. 8123

18. Air Dryer & Cleaner - U.S. Government Property No. 038

19. AC Milliammeter - Simpson - 0-10 ma

20. AC Milliammeter - Simpson - 0-50 ma

21. Manometer - Central Scientific 0-760 mm of Hg

22. Tesla Coil - Central Scientific - BD No. 10

REFERENCES

1. "Investigation of Secondary Phenomena for Use in Checkout" Technical Documentary Report No. APL-TDR-64-4, Jan. 1964.

2. Klauss, Philip., "Potential Failures Detected by Radio Frequency Noise" Aviation Week and Space Technology, Jan. 7, 1963.

3. Jones, Prof. F. Llewellyn, "Initiation of Discharges at Electrical Contacts" Institute of Electrical Engineers 100 Part I, 169(1953).

4. Crowther, J. A., "Ions, Electrons, and Ionizing Radiations," Fourth Edition, Lonymans Green & Co. (New York, 1924).

5. Ward, A. L., "Calculations of Electrical Breakdown in Gases" TR-1193, Harry Diamond Fuse Labs., (Washington 25, D.C., Attention AMXDO-RD-930, 10 January 1964).

6. Loeb, Leonard B., "Basic Processes of Gaseous Electronics," University of California Press (Berkeley California, 1960).

7. Loeb, Leonard B., "Recent Advances on Streamers in the Author's Laboratory", Department of Physics, University of California, Berkley, Cal.

8. Nasser, E., "The Nature of Negative Streamers in Spark Breakdown", Dielectrics Vol. 1, No. 2c, Heywood & Co. Ltd., London, England 1963.

9. Loeb, L. B., Westberg, R.G., Huany, H.C. "Streamer Mechanisms in Filamentary Spark Breakdown in Argon Photomultiplier Techniques", Physical Review, 123, pp. 43-50(1961).

10. Nasser, Essam, Loeb, Leonard B., "Impulse Streamer Branching from Lichtenberg Studies, Journal of Applied Physics 34, pp. 3340-3348, November, 1963.

11. Raether, H., "Electron Avalanches and Breakdown in Gases", p. 3 et seq. Butterworth Inc., 7235 Wisconsin Avenue, Washington, D.C. 20014.

12. Schlumbohm, H.Z. Phys. $\underline{159}$, 212, (1960).

13. Loeb, Leonard B., "Basic Processes of Gaseous Electronics", University Press, Los Angeles, California, 1960, p. 760.

14. Gray, Dwight, et al, "American Institute of Physics Handbook", McGraw-Hill Book Co., Inc., New York - 1957, p. 5-168.

15. Jnanananda, Swami, "High Vacua, Principles, Production and Measurement", D. Van Nostrand Co., Inc., New York (1947) p. 31.

16. Gray, Dwight E., "American Institute of Physics Handbook" 1957, p. 5-74, McGraw-Hill Book Co., Inc., New York.

17. Holm, Ragnar, "Electric Contacts Handbook", Springer-Verlag Berlin/Gottingen/Heidelberg, Germany, 1958.

18. Ohmite Mfg., Co., 3635 W. Howard St., Skokie, Ill. 60076.

19. International Resistance Co., 401 North Broad St., Philadelphia, Pa. 19108.

20. National Carbon Co., Cleveland, Ohio.